ceramics

MDPI

Review

Additive Manufacturing of Ceramics and Ceramic-Based Composites: Processing, Properties, and Engineering Applications

Subin Antony Jose, John Crosby and Pradeep L. Menezes *

Department of Mechanical Engineering, University of Nevada, Reno, NV 89557, USA; subinj@unr.edu (S.A.J.); johncrosby@unr.edu (J.C.)
* Correspondence: pmenezes@unr.edu

Abstract

Ceramics are widely evaluated for their extreme hardness, high-temperature stability, and corrosion resistance, which enable applications in harsh service environments. However, these same properties, high melting points, brittleness, and low thermal shock resistance, make conventional manufacturing of complex ceramic components difficult and expensive. Traditional processes often require costly diamond tooling or energy-intensive sintering and tend to produce only simple geometries, with significant waste material and risk of defects. Additive manufacturing (AM) has recently emerged as a promising route to fabricate intricate, near-net-shape ceramic parts without these drawbacks. By building components layer by layer, AM reduces the need for extensive machining and enables the fabrication of geometrically complex, near-net-shape ceramic structures with reduced material waste, although challenges such as porosity, interlayer defects, and cracking during post-processing remain. Nonetheless, ceramic AM technologies lag behind their metal and polymer counterparts, and significant challenges remain in achieving fully dense parts with reliable mechanical properties. This review provides an in-depth overview of the state of the art in ceramics and ceramic composite additive manufacturing. We detail the most widely used AM processes (stereolithography, binder jetting, material extrusion, powder bed fusion, inkjet printing, and direct energy deposition) and typical feedstock formulations for each technique. We examine the resulting mechanical properties (strength, toughness, hardness, wear resistance) and functional properties (thermal stability, dielectric behavior, biocompatibility) of additively manufactured ceramics, and discuss their current and potential engineering applications in the aerospace, defense, automotive, biomedical, and energy sectors. Persistent challenges, including porosity, shrinkage and cracking during sintering, achieving uniform microstructures, high process costs, and scalability issues, are analyzed, and we highlight promising future directions such as multi-material grading, integration of machine learning for process optimization, and sustainable manufacturing approaches. Despite significant progress, challenges remain in achieving fully dense structures, improving process reliability, and scaling ceramic AM for industrial applications, highlighting the need for further research in process optimization, material design, and multi-material integration.

Keywords: additive manufacturing; ceramic materials; ceramic matrix composites; mechanical properties; functional properties; densification; engineering applications

Check for updates

Academic Editors: Bartolomeo Coppola, Frank Kern and Julien Schmitt

Received: 23 January 2026
Revised: 13 April 2026
Accepted: 16 April 2026
Published: 22 April 2026

Copyright: © 2026 by the authors. Licensee MDPI, Basel, Switzerland. This article is an open access article distributed under the terms and conditions of the Creative Commons Attribution (CC BY) license.

1. Introduction

Ceramics are typically defined as inorganic, non-metallic materials characterized by high thermal stability, hardness, and chemical resistance. In addition, advanced processing routes such as polymer-derived ceramics have expanded this class by enabling alternative pathways to achieve similar functional properties. Their high melting temperatures and low thermal expansion make them ideal for high-temperature applications [1–3]. For example, in heat exchangers, rocket nozzles, gas turbine blades, brake rotors, and thermal protection systems, where metals would oxidize or creep [4]. Likewise, the extreme hardness of many ceramics (e.g., alumina, silicon carbide) yields outstanding wear resistance [5–7], beneficial in abrasive environments such as blasting nozzles, cutting tools, bearings, and seals [8,9]. Ceramics also exhibit excellent corrosion resistance and are employed as protective linings or coatings in chemical processing equipment, nuclear reactors [10], and wastewater treatment systems [11]. Despite these attractive properties, the use of ceramics in advanced applications has been highly constrained by manufacturing limitations. The very characteristics that make ceramics desirable, including extreme hardness, brittleness, and refractory nature, render them difficult to shape using conventional methods. For instance, ceramics cannot be easily cast or welded like metals due to their high melting points and poor thermal shock resistance [12,13]. Processes like uniaxial or isostatic pressing are typically limited to simple geometries and produce substantial material waste [14]. Machining fully sintered ceramics into complex forms is often prohibitively expensive, requiring diamond tooling and resulting in low material removal rates and potential surface damage [15].

In recent years, additive manufacturing (AM) of ceramics and ceramic-based composites has emerged as a compelling solution to many of these challenges. By building parts layer-by-layer from a digital design, AM eliminates the need for extensive subtractive machining of hard ceramics and enables rapid prototyping of intricate shapes that would be impossible or very inefficient with traditional methods. For example, complex lattice structures, internal cooling channels, and functionally graded compositions can be achieved in ceramic components via AM, greatly expanding design freedom in high-temperature or wear-critical devices. Most importantly, additive techniques can produce near-net shape parts that are almost fully dense and defect-free after post-processing, preserving the inherent strength of the ceramic material in the final component [13].

Nevertheless, ceramic AM is still a developing field and faces numerous challenges before it can be widely adopted for mass production. Many ceramic AM processes find it difficult to achieve the same density and mechanical performance as conventional sintering, often requiring extensive post-build sintering or infiltration steps to eliminate porosity. Feedstocks for ceramic AM (such as powder/binder mixtures or photocurable slurries) must be carefully formulated to ensure printability and uniformity, as issues like particle agglomeration or non-homogeneous binder distribution can introduce flaws in the printed part. The use of temporary binders and additives means printed "green" parts often undergo substantial shrinkage or distortion during binder removal and sintering, which can lead to cracking or shape inaccuracy if not properly controlled. Additionally, current ceramic AM equipment can be costly and slow, and the processes are not yet easily scalable to high-throughput manufacturing in the way metal powder-bed fusion has become in some industries. Reliability and repeatability are also concerns; achieving consistent microstructure and properties across multiple builds or machines is an area of active research [1].

This review provides a comprehensive examination of the state of the art in ceramic additive manufacturing and addresses these considerations. Section 2 offers an overview of the major AM techniques for ceramics, including vat photopolymerization (stereolithography), binder jetting, material extrusion (robocasting and fused deposition), powder bed

fusion (laser sintering/melting), inkjet printing, and directed energy deposition, comparing their principles, advantages, and limitations. Section 3 discusses typical feedstocks for these processes (pure oxide and non-oxide ceramics, ceramic–polymer suspensions, cermets, and pre-ceramic polymers), highlighting how particle characteristics and binder systems influence printability and final part quality. Section 4 describes key post-processing stages such as debinding, sintering (including advanced methods like hot pressing and spark plasma sintering), and infiltration, and their effects on densification and microstructure. Section 5 evaluates the mechanical (strength, toughness, hardness) and functional properties (thermal shock resistance, dielectric loss, optical behavior, and biocompatibility) of additively manufactured ceramics reported in the literature, in some cases comparing them to conventionally made counterparts. Section 6 then surveys current and emerging engineering applications of ceramic AM across mechanical engineering domains, including aerospace/defense (for lightweight heat-resistant parts and armor), automotive (for catalytic converters and engine components), biomedical (for dental and bone implants), and energy/electronics (for fuel cells and electromagnetic devices). In Section 7, we discuss the remaining challenges impeding wider adoption of ceramic AM, such as residual porosity and cracks, achieving uniform microstructures, process cost and scalability, and part reliability. In Section 8, we explore future directions that are poised to address these issues. These include the development of multi-material and functionally graded ceramic components via AM, the integration of artificial intelligence and machine learning to optimize designs and printing parameters, and strategies for more sustainable processing and recycling in ceramic AM. Finally, Section 9 concludes with an outlook on how continued innovation in materials, processes, and process control will enable additive manufacturing to become a mainstream production route for advanced ceramic components.

Compared to existing review articles on ceramic additive manufacturing, the present work provides a more integrated perspective by linking processing techniques with feedstock design, post-processing strategies, and resulting mechanical and functional properties. In particular, recent developments over the past five years are emphasized, including advances in high-solid-loading feedstocks, multi-material and functionally graded printing, and emerging post-processing approaches such as spark plasma sintering and hybrid densification techniques. Furthermore, this review highlights the relationships between processing parameters, microstructure evolution, and performance, offering a more application-oriented understanding of ceramic AM systems.

2. Overview of Additive Manufacturing Techniques for Ceramics

AM encompasses several distinct process families, and nearly all have been adapted in some form to fabricate ceramic parts. The American Society for Testing and Materials (ASTM) broadly classifies AM processes into seven categories; of these, six methods have demonstrated success in producing usefully dense, high-quality ceramic components. They are vat photopolymerization (stereolithography), binder jetting, material extrusion (including fused deposition of ceramic filaments and direct ink writing/robocasting of pastes), powder bed fusion (selective laser sintering/melting), material jetting (ceramic inkjet printing), and direct energy deposition [16]. Table 1 provides a comparison of these AM methods, their feedstocks, and process characteristics. Regardless of the specific technique, ceramic AM generally follows a similar workflow (illustrated schematically in Figure 1). This figure highlights the sequential stages involved in ceramic AM, emphasizing the critical role of post-processing in achieving final densification and mechanical integrity. It should be noted that the schematics presented illustrate the general AM process principles, while post-processing routes vary significantly depending on material systems and application requirements. A 3D CAD model is first prepared and discretized into layers, suitable

feedstock is chosen or formulated, and process parameters (e.g., toolpaths, layer thickness, binder deposition or laser power, etc.) are then applied to build the part layer-by-layer. The initial "green" part typically contains binders or other sacrificial phases and is not yet fully dense or strong, so after printing, it undergoes post-processing such as curing, debinding (burning out organic components), and sintering to yield the final fully ceramic part. In some cases, additional steps like infiltration with a second phase or hot isostatic pressing may be used to further densify or strengthen the part. Below, we summarize the principles and notable features of each major ceramic AM method.

Table 1. Comparison of AM methods used to manufacture ceramic parts.

AM Method	Feedstock	Printing Mechanism	Green Part Strength	Printing Accuracy	Build Rate	Required Post-Processing	References
Stereolithography	Ceramic powder suspended in UV curable resin	UV laser cures liquid resin into solid part	Medium-Low	High (~25–100 µm)	Low–Moderate	Pyrolysis to remove resin, sintering	[17,18]
Binder Jetting	Loose ceramic powder, liquid binder	Print head jets binder onto powder bed	Low	Moderate (~50–200 µm)	High	Curing, debinding, sintering	[19]
Material Extrusion	Solid filament, pellets, or shear-thinning liquid	Feedstock is extruded through nozzle	Medium	Moderate (~100–500 µm)	Moderate	Curing, debinding, sintering	[13,20]
Powder Bed Fusion	Loose ceramic powder	Laser scans across powder bed, fuses powder	Medium-High (SLS), High (SLM)	High (~50–150 µm)	Moderate	Sintering	[13,21]
Inkjet Printing	Colloidal ceramic + binder suspension	Ceramic ink is directly jetted onto build platform	Low	Very High (~20–50 µm)	Low	Curing, debinding, sintering	[22]
Direct Energy Deposition	Ceramic powder, composites	Powder fed into focal point of laser, directly fused to part	High	Low–Moderate (~200–500 µm)	High	None, optional surface machining	[23,24]

Note: The terms low, medium, and high green strength refer to the relative mechanical integrity of the as-printed (unsintered) parts, indicating their ability to withstand handling before post-processing.

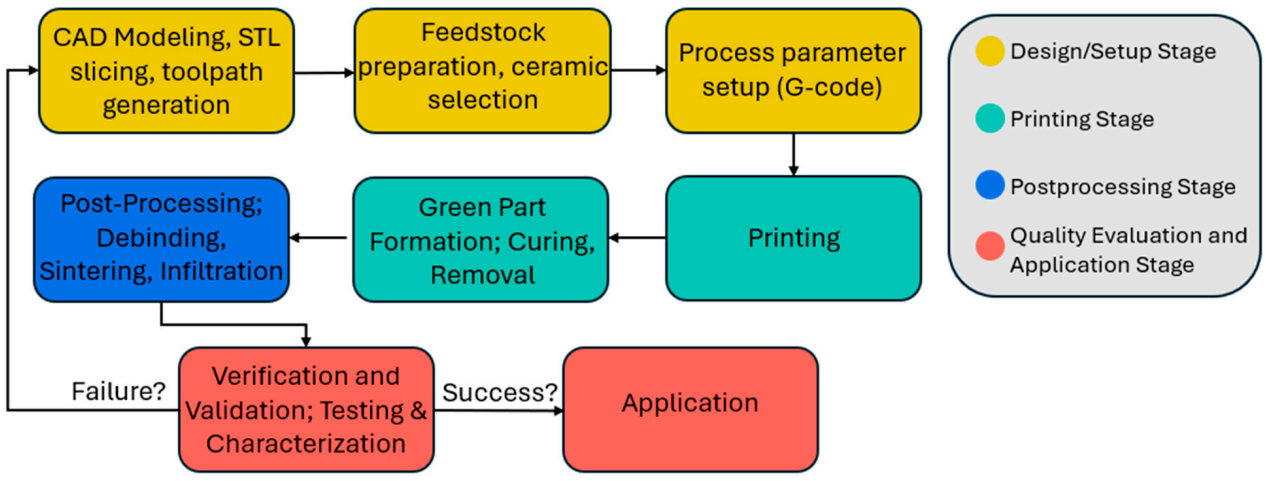


Figure 1. Flowchart detailing the general AM process.

2.1. Stereolithography/Vat Photopolymerization

Stereolithography/vat photopolymerization uses ceramic powder suspended in a UV-curable liquid resin as feedstock. Printing is carried out using a UV laser (or projector) that selectively cures the liquid resin into a solid polymer/ceramic composite layer by layer. Complex 3D shapes are built up as the laser scans the cross-section of each layer and solidifies the slurry locally. The green strength obtained would be medium–low, since the printed part ("green body") is held together by the polymerized resin, so it is fragile and must be handled with care. As post-processing, a critical post-step is pyrolysis to burn out the photopolymer binder, leaving behind a porous ceramic object, followed by sintering to consolidate the ceramic particles into a dense part. Stereolithography is capable of very high resolution and fine feature detail (on the order of tens of microns) because of the precision of photopolymerization. Key challenges include formulating the slurry with high ceramic loading (to minimize shrinkage) while retaining suitable viscosity, dispersion, and cure depth [25]. However, limitations include high slurry viscosity at high solid loading, potential shrinkage during debinding and sintering, and relatively low build rates. Despite these challenges, ceramic stereolithography has produced parts with excellent surface quality and mechanical properties, for example, flexural strengths of ~500–600 MPa in alumina after sintering have been reported. A schematic diagram of the stereolithography process is shown in Figure 2.

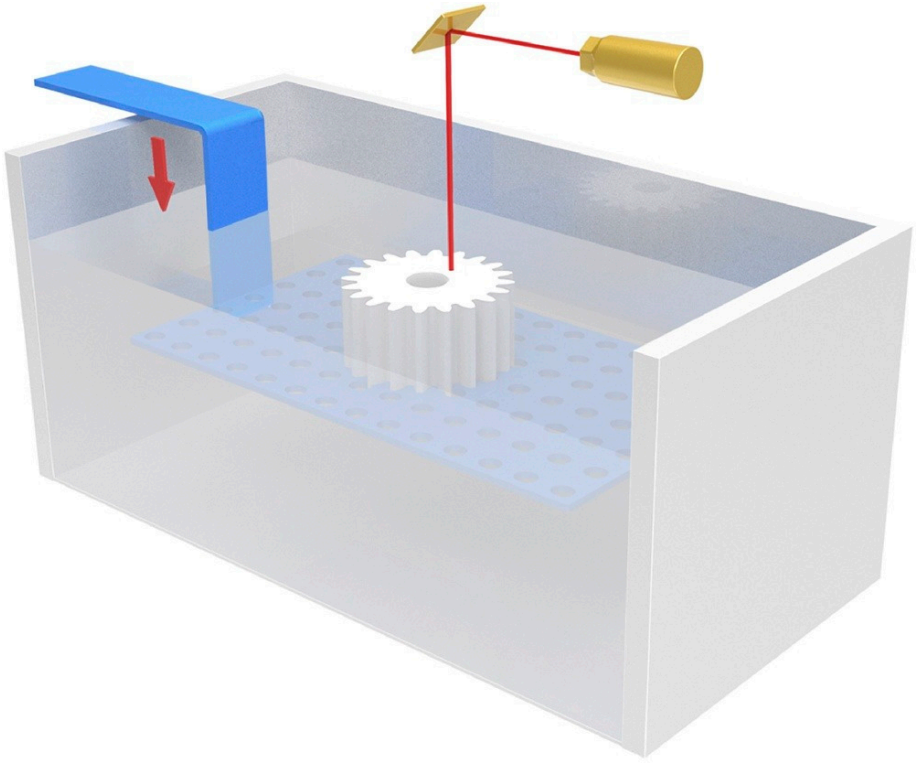


Figure 2. Schematic diagram of the stereolithography process. Reproduced from [26], open access.

2.2. Binder Jetting

Loose ceramic powder in a bed and a liquid binder solution are used as the feedstock for binder jetting. Printing is carried out as the inkjet print head selectively drops binder onto each powder layer in the shape of the cross-section, adhering to the ceramic particles where the binder lands. After one layer is printed, the powder bed is lowered, and a new layer of powder is spread by a roller, then the binder is jetted again, and so on [16]. It has low green strength, since the printed part is a "green body" made of loosely glued powder with minimal strength. It must remain surrounded by unbound powder until

cured to avoid collapse. Binder-jetted parts require extensive post-processing. First, a curing step (often gentle heating) solidifies or polymerizes the binder [27]. Next, the cured part is carefully removed from the powder bed and undergoes debinding (burning out the binder) and then sintering to fuse the particles into a dense ceramic. Often, the sintered density is <100%, so additional infiltration with a molten metal or glass may be used to fully densify the part. Binder jetting offers one of the fastest build rates among ceramic AM methods and can produce large parts. However, the use of binders and the two-step (print then sinter) process can lead to considerable shrinkage (10–30%) and porosity if not optimized. Maintaining uniform binder distribution and avoiding large pore formation during debinding are key to obtaining defect-free parts with this method. However, binder jetting suffers from low green strength, significant shrinkage, and challenges in achieving full density without extensive post-processing. A diagram showing the process flow of the binder jetting process is shown in Figure 3.

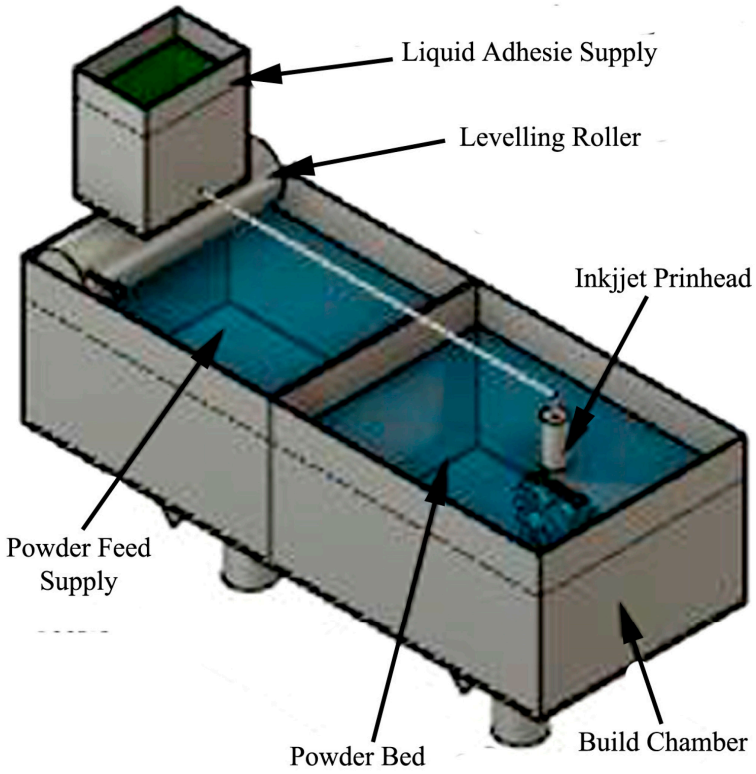


Figure 3. Process flow diagram for AM with binder jetting. Reproduced from [28], open access.

2.3. Material Extrusion (Including Fused Filament Deposition and Robocasting)

The feedstock for material extrusion is a ceramic-loaded thermoplastic filament or a paste-like slurry with high solid content [29]. The material is fed through a nozzle (by a filament drive gear, a piston/plunger, or a screw) and deposited line by line to form each layer [30]. In fused deposition modeling (FDM, [31]) style, a filament made of ceramic powder mixed with a thermoplastic binder is melted and extruded, whereas in direct ink writing, a shear-thinning ceramic paste is extruded at room temperature. The printed filament or bead solidifies quickly (by cooling or solvent evaporation), so the part can hold its shape layer by layer. Green strength is medium, since the polymer binder in the filament or paste provides some strength to the "green" part after extrusion, though complex shapes may require printed support structures or carefully tuned rheology to prevent distortion. Typically, the printed part is first cured (if a paste was used) or simply allowed to cool/harden. Then, the binder is removed via slow heating (thermal debinding),

and the remaining ceramic structure is sintered to full density. Material extrusion is one of the more accessible ceramic AM methods, since it can use relatively inexpensive equipment (modified FDM printers or syringe extruders). Recent work has shown that high loadings of ceramic (50–60 vol% solids) in filament or paste form can be achieved, enabling sintered strengths comparable to pressed ceramics (e.g., ~700 MPa flexural strength in zirconia). Despite its accessibility, the process is limited by lower resolution and challenges in maintaining dimensional accuracy due to rheological constraints. A key challenge is optimizing the rheology of the feedstock. It must be fluid enough to extrude but solid-like enough to hold the shape after deposition. Robocasting has successfully produced dense structures, including oriented fiber-reinforced composites and hierarchical porous scaffolds by leveraging tailored ink chemistry [32]. A schematic of material extrusion (fused deposition) of ceramic paste is shown in Figure 4.

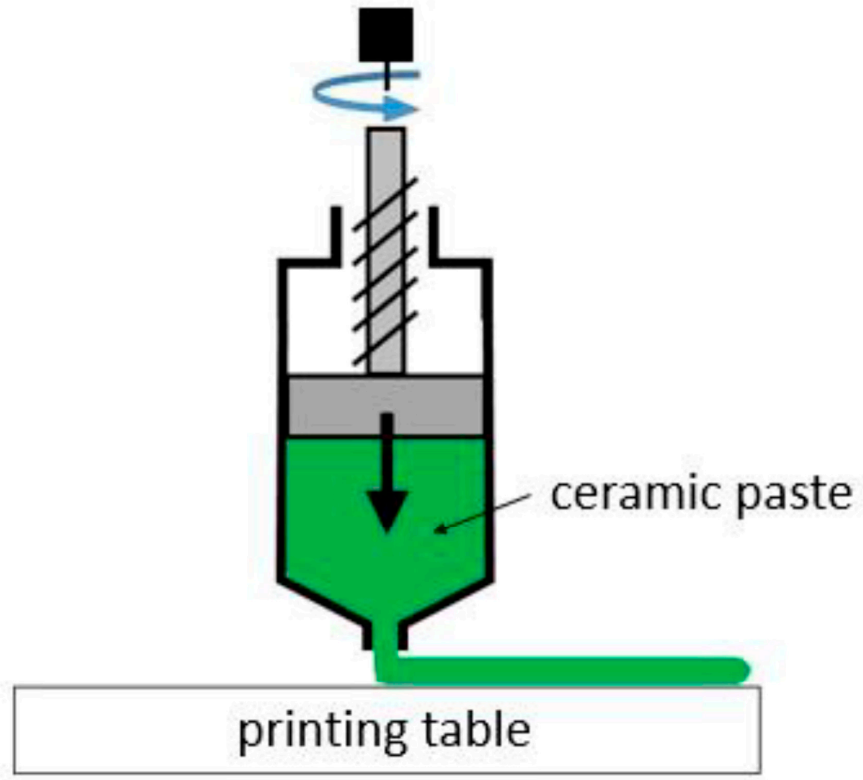


Figure 4. Schematic of material extrusion of ceramics. Reproduced from [33], open access.

2.4. Powder Bed Fusion (Selective Laser Sintering/Melting)

In this process, fine ceramic powder is spread into thin layers as feedstock. Printing is performed as a high-power laser beam scans each powder layer according to the cross-section geometry. In selective laser sintering (SLS), the laser locally heats particles (below their melting point) to induce solid-state sintering necks between them. In selective laser melting (SLM), a more powerful laser fully melts the ceramic powder in each scanned area, which then re-solidifies upon cooling. The process is typically carried out in an inert gas atmosphere to prevent oxidation or decomposition of the ceramic during the high-temperature exposure. Unfused powder supports the part during building. Green Strength is medium to High. In SLS, the green part is a partially sintered solid and can have moderate strength (sufficient to be handled), while in SLM, the part is already a fully melted and solidified ceramic, theoretically providing high strength even before post-processing. SLS parts generally require a furnace sintering cycle after printing to increase density and mechanical properties, since laser-sintered ceramics may only reach ~70–90% density

as-printed. SLM parts, having been melted, can achieve high density (~99%) in situ [34], though in practice, ceramics' tendency to crack under thermal stress means that fully dense SLM of ceramics is challenging [35]. To mitigate cracking, researchers have experimented with smaller layer thicknesses, preheating the powder bed, or using composite powders. However, some residual porosity or microcracks may still require healing via post-sintering or hot isostatic pressing. Powder bed fusion has the advantage of producing parts with no binder (especially in SLM), eliminating a debinding step and often resulting in superior as-printed strength compared to other methods. However, extremely high temperatures and rapid cooling can introduce thermal stresses or phase changes in ceramics (which lack the ductility of metals to relieve stress), making process optimization critical for crack-free results. A schematic of the laser-based powder bed fusion process is given in Figure 5.

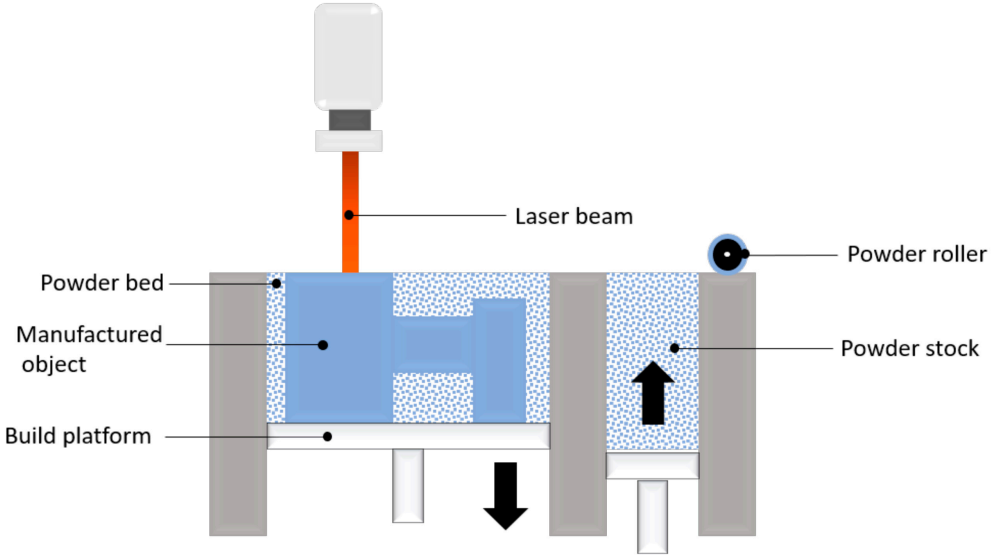


Figure 5. Schematic of the laser-based powder bed fusion process. Reproduced from [36], open access.

2.5. Material Jetting (Ceramic Inkjet Printing)

A liquid ink containing dispersed ceramic nanoparticles and often a binder or precursor is the feedstock, which solidifies upon drying. A print head deposits a fine droplet of the ceramic ink in a patterned manner onto a substrate (or onto previous layers). The solvent in the droplets evaporates either naturally or under heat or UV, leaving behind solid ceramic deposits that make up the layer. There are several sub-modes (continuous vs. drop-on-demand inkjet, piezoelectric vs. thermal drop ejection) used to control the droplet formation [37,38]. Inkjet printing can create complex 2D or 3D ceramic patterns with very high resolution (feature sizes in the tens of microns) and is particularly useful for multi-material printing by using multiple inks. Green strength is low because the printed object consists of loosely bound ceramic particles with minimal structural integrity until further processing. Handling must be delicate, and often the part is built on a support substrate. After printing, the part is typically dried thoroughly and then undergoes thermal debinding to remove any organic components of the ink. A final sintering step densifies the ceramic. Achieving uniform shrinkage is challenging because the layer-wise drying can lead to internal stresses or differential density regions if not handled properly. Nonetheless, inkjet-based AM has successfully fabricated intricate structures like photonic crystals and dental implants in ceramics. A major limitation is the need for low-viscosity inks, which restricts the solid loading and thus causes significant shrinkage upon sintering (often 20–30%). Breakthroughs in colloidal chemistry that allow higher ceramic content inks

or novel curing strategies (e.g., using a reactive binder) are being actively researched to improve this technique. Figure 6 shows a schematic diagram of the material jetting process.

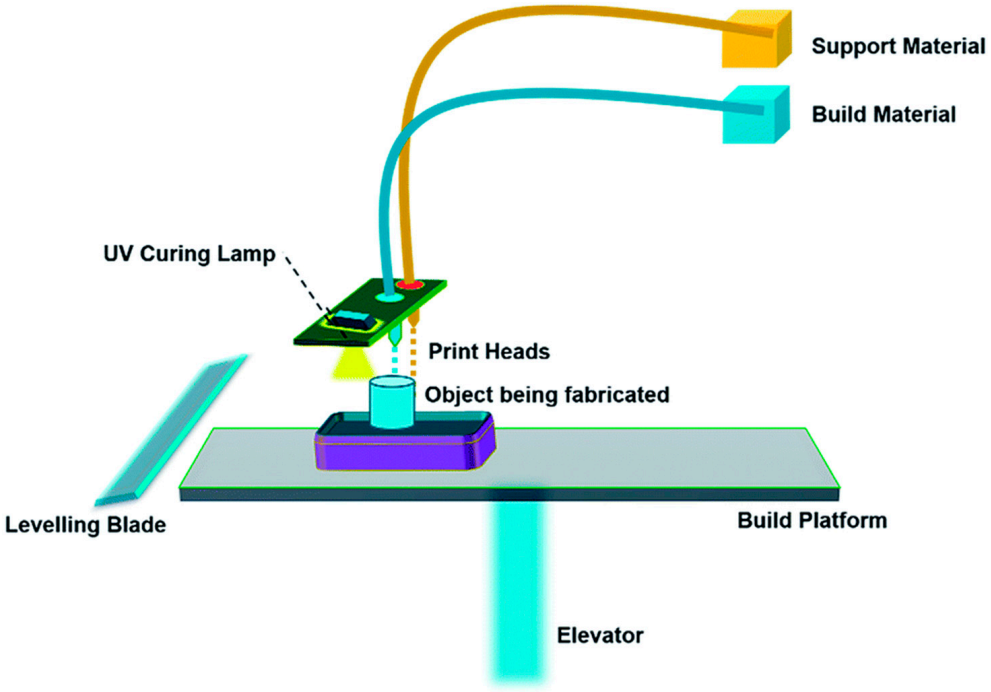


Figure 6. Schematic diagram of the material jetting process. Reproduced from [39], open access.

2.6. Direct Energy Deposition (DED)

Typically, a ceramic powder (or a powder-wire combination for composites) is the feedstock for the process. Printing is performed using a focused energy source (usually a high-power laser or electron beam) that creates a molten pool on a substrate, and ceramic powder is simultaneously fed into this molten pool. The powder particles melt (or at least partially melt) upon entering the pool, and then the molten material solidifies and bonds to the substrate as the heat source moves away. This process is repeated in toolpath patterns to build up layers (often on an existing part or platform). DED is essentially a form of precision welding for ceramics. Green strength is high because the ceramic is consolidated by melting, and the deposited material is solid and strongly bonded immediately after deposition. No binder is involved, so the as-built part is a fully ceramic structure requiring no curing. Although DED can produce relatively dense structures, additional post-processing such as annealing is often required to relieve residual stresses and mitigate cracking, particularly for ceramic materials [13]. Surface machining may be applied to achieve dimensional tolerances [40]. DED can produce very dense parts and is unique in enabling functionally graded compositions by feeding multiple powders through different nozzles. However, applying DED to ceramics is extremely challenging due to their low thermal shock resistance, which means ceramic DED runs the risk of crack formation under steep thermal gradients during rapid melting/solidification cycles. Recent studies have shown that careful control of laser parameters (power, scan speed) and powder feed rate can mitigate these issues. For example, depositing ceramic in very small increments or onto a pre-heated substrate helps avoid cracking [41]. DED has been successfully used for the repair or addition of material to existing ceramic structures, and to create novel ceramic–metal composites (cermets) by co-deposition of metal and ceramic powders. Figure 7 shows a schematic diagram of the DED process.

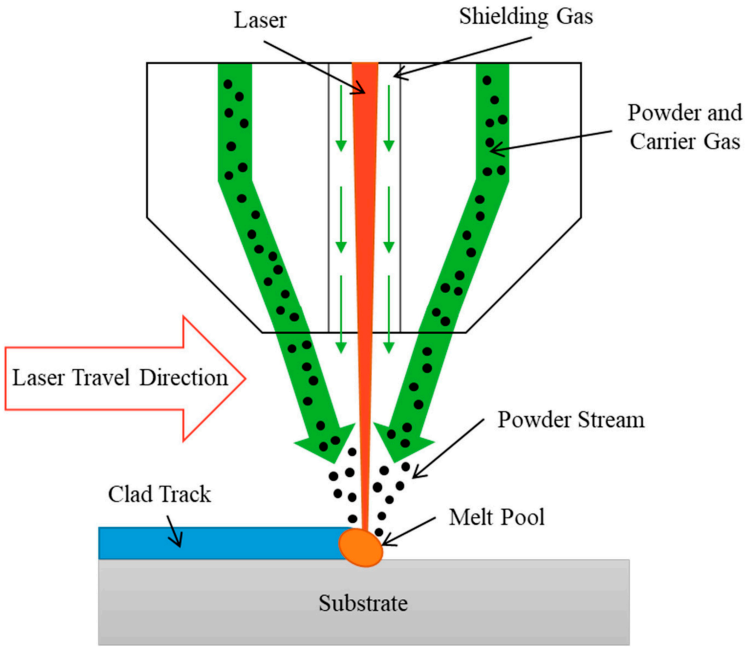


Figure 7. Schematic diagram of the DED process. Reproduced from [42], open access.

To provide a clearer comparative perspective, the major additive manufacturing techniques for ceramics can be broadly categorized based on processing principles and performance trade-offs. Vat photopolymerization and inkjet printing offer high resolution but are limited by lower build rates and complex post-processing. Binder jetting provides high productivity and scalability but suffers from lower green strength and higher porosity. Material extrusion offers cost-effective processing with moderate resolution, while powder bed fusion and direct energy deposition enable higher density, but face challenges related to thermal stresses and process stability. This comparative framework highlights that no single technique is universally optimal, and process selection depends strongly on material system, required resolution, and application-specific performance requirements.

To provide a clearer understanding of the process pathways associated with different additive manufacturing techniques, Figure 8 summarizes the sequence of steps from feedstock preparation to final densification for representative ceramic AM processes.

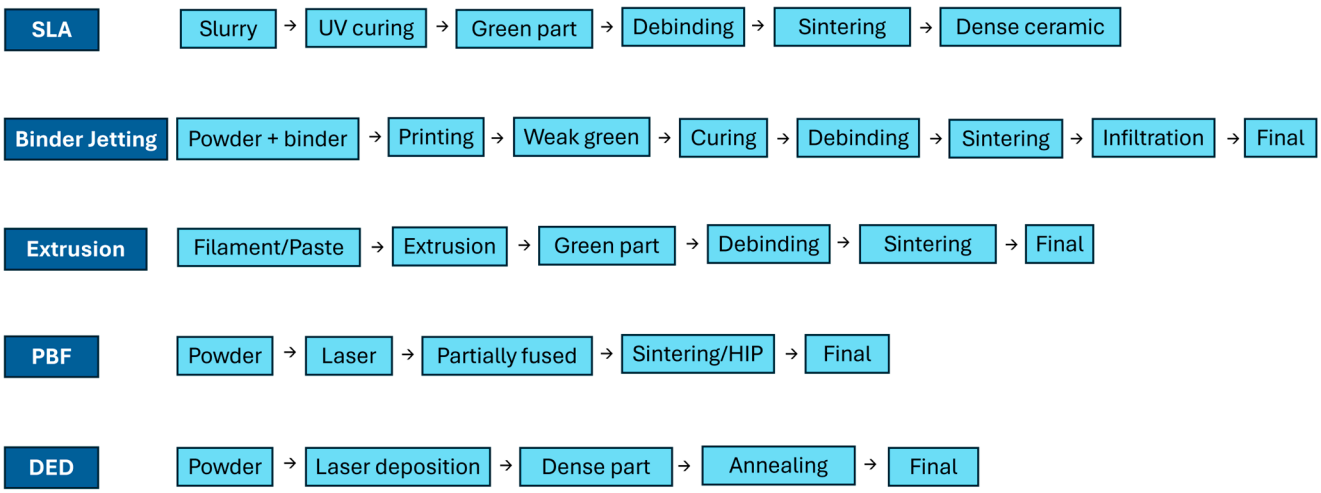


Figure 8. Schematic representation of process pathways in ceramic additive manufacturing, illustrating the sequence from feedstock preparation to green part formation and subsequent post-processing steps.

3. Ceramic and Composite Feedstocks for AM

Successful AM of ceramics hinges on the development of suitable feedstock materials that meet the process requirements (flow behavior, curing characteristics, etc.) while yielding excellent final properties. Ceramic AM feedstocks can be broadly categorized into three groups: pure ceramics (oxide or non-oxide ceramics in powder form), ceramic–polymer composites (including pre-ceramic polymers and slurry resins), and ceramic–metal composites (cermets). Table 2 lists some common ceramics used in AM and their properties. Each AM technique imposes specific demands on feedstock properties such as viscosity (for extrusion or jetting), particle size distribution (for powder spreading or slurry stability), and binder content (for adequate green strength vs. ease of removal). Regardless of process, a recurring goal is to maximize the ceramic solid loading to minimize shrinkage during sintering while maintaining printability. For instance, vat photopolymerization slurries and extrusion pastes often contain ~45–60 vol% ceramic solids, and binder jet powders are often bimodal mixtures to improve packing density [43]. In this section, we discuss feedstock design for major ceramic systems, including alumina, zirconia, silicon carbide, silicon nitride, cermets, and pre-ceramic polymers, highlighting how particle characteristics and binder chemistry affect the additive manufacturing process and the quality of printed parts.

Table 2. Mechanical properties and characteristics of pure ceramics when produced via additive manufacturing.

Ceramic	Chemical Formula	Type	Density [g/cm^3]	Vickers Hardness [GPa]	Flexural Strength [MPa]	References
Alumina	Al_2O_3	Oxide	3.97	18	500–600	[44]
Zirconia	ZrO_2	Oxide	5.65	11.5	490	[45]
Silicon Carbide	SiC	Non-Oxide	3.21	18	675	[46]
Silicon Nitride	Si_3N_4	Non-Oxide	3.71	13.8	700–770	[47]

3.1. Pure Oxide Ceramics (Alumina, Zirconia)

Alumina (Al_2O_3) is the most studied AM ceramic. It is an oxide with a high melting point (~2072 °C) and is often used as a benchmark for ceramic processing methods [48]. Successful alumina feedstocks have been prepared for nearly all AM techniques. A key factor is achieving high solids loading while retaining manageable rheology. For example, in direct ink writing, Chan et al. [49] formulated an alumina emulsion ink and showed that the storage modulus and yield stress of the ink directly impacted printability and whether printed structures retained their shape. Too low a yield stress led to parts slumping, while too high a stress made extrusion difficult. By tuning surfactant and oil content, they achieved a printable window where the ink behaved solid-like at rest but flowed under pressure. In stereolithography, the dispersant and monomer chemistry strongly influence viscosity and cure depth. Han et al. [50] showed that optimizing the dispersant in an alumina photopolymer slurry improved the cured strength of green parts and the compression strength of sintered alumina up to ~125 MPa. Achieving fine particle dispersion is critical as well. Shahed et al. [51] found that using a bimodal alumina powder (with fine particles to fill interstices between coarse ones) improved powder packing in binder jetting. However, if the size ratio was too large, the fine particles segregated and caused density variations. Alumina parts additively manufactured by optimized feedstocks can attain flexural strengths on the order of 500–600 MPa and Vickers hardness around 18 GPa after proper sintering [52].

Zirconia (ZrO_2), usually stabilized with 3 mol% yttria (3YSZ) for phase stability, is another popular oxide ceramic in AM, particularly for biomedical implants due to its

biocompatibility and high toughness. Zirconia's behavior in feedstocks can differ from alumina's. For instance, it often requires different dispersants or binder formulations because of its higher density and different surface chemistry. Yu et al. [45] developed a water-based YSZ feedstock for a screw-extrusion process and achieved high Vickers hardness (~11.5 GPa) and bending strength (~490 MPa) in the sintered parts. Importantly, they noted that fine zirconia powders increased slurry viscosity significantly, so dispersant optimization was key to loading ~45 vol% solids while keeping the paste extrudable. A common strategy to improve the toughness of printed zirconia is to incorporate alumina as a second phase, creating a zirconia–alumina composite that leverages zirconia's transformation toughening and alumina's stiffness [53]. For example, Liu et al. [54] investigated zirconia-toughened alumina (ZTA) composites fabricated via stereolithography, demonstrating that sintering conditions significantly influence hardness and strength. Managing the different shrinkage of two phases is challenging, but can be addressed by careful particle sizing and matching sintering profiles. Another study by Kuang et al. [55] varied oligomer content in a zirconia UV-curable resin and found an optimal balance where viscosity was low enough to print, yet cured parts had sufficient strength; too much oligomer improved photo-curing but made the slurry too viscous to process.

3.2. Pure Non-Oxide Ceramics (Silicon Carbide, Silicon Nitride)

Non-oxide ceramics like SiC and Si_3N_4 are highly desirable for extreme environments (e.g., semiconductor processing, armor, and high-temperature engines) but are notoriously difficult to process because they oxidize during conventional sintering. AM of these often involve either protective atmospheres or pre-oxidizing the feedstock [56]. Bai et al. [57] reported that SiC strongly absorbs UV light, reducing the cure depth in stereolithography, limiting layer thickness. Tang et al. and Cao et al. tackled this by pre-oxidizing SiC powder to form a thin SiO_2 layer; this increased UV transparency, allowing thicker curing in each layer [58,59]. During the post-processing, they introduced a carbothermal reduction step to remove the silica in situ and recover SiC, resulting in dense SiC parts. Similarly, Yang et al. [47] pre-oxidized Si_3N_4 powder and added a silane coupling agent to improve dispersion in a DLP resin, achieving a significant reduction in slurry viscosity and producing Si_3N_4 parts with ~14 GPa hardness and ~700 MPa bending strength, which is comparable to conventionally pressed Si_3N_4 implants [60]. These studies underscore that for non-oxides, controlling oxygen exposure during printing and sintering is critical; using inert atmospheres for debinding/sintering or sacrificial getters can prevent excessive oxidation that would degrade properties. Ding et al. [61] printed SiC mirror prototypes via stereolithography, followed by a multi-step post-process (burnout, partial sintering, polymer infiltration, final sintering) and obtained ~93.5% density in the end. Kong et al. [62] introduced a novel "powder extrusion printing" for SiC, where a feedstock of SiC powder and polymer binder is extruded as small pellets (3–5 mm) that are then deposited by a screw. This allowed them to print without fully melting a filament, possibly improving uniformity for large cross-sections. In all these cases, fine control of particle size is vital. Li et al. [63] showed that in direct ink writing of SiC, a multimodal particle distribution could improve flow and packing, but too many ultrafine particles caused flocculation, indicating an optimal mix is needed.

3.3. Ceramic–Metal Composites (Cermets)

Cermets combine a ceramic matrix with a metal binder (often Ni, Co, or Fe) to improve fracture toughness and facilitate sintering. Tungsten carbide–cobalt (WC–Co) is a classic cermet used for cutting tools and has been studied in binder jetting and extrusion contexts. A major concern for cermet feedstocks is differential sintering: the metal can

significantly enhance densification by liquid phase sintering, but also can cause distortion if not uniformly distributed. Enneti and Prough prepared a WC–12%Co feedstock for binder jetting and showed that, after debinding and sintering, they could achieve dense structures with wear resistance comparable to conventionally made ones [64]. Davydova et al. [65] improved a boron carbide feedstock by chemically depositing a 2% Co layer on B_4C powder particles, ensuring better wetting and densification during laser sintering. For powder bed fusion or DED, the wettability of the metal on the ceramic is crucial. A low contact angle between molten metal and ceramic promotes infiltration and bonding. Vedel et al. [66] measured that Fe, Co, and Ni exhibit reasonably good wetting on carbides like TiC, suggesting those metals are suitable binders for carbide composites printed by methods like DED or inkjet with subsequent melt infiltration. In filament-based extrusion, feedstocks of ceramic–metal often use a fine metal powder mixed with ceramic powder and binder. The presence of metal can actually aid sintering by triggering transient liquid-phase sintering at relatively lower temperatures. The challenge is avoiding reactions between the metal and ceramic that could form brittle compounds (for instance, Ni with SiC can form nickel silicide). Thus, sintering atmospheres and heating profiles must be tuned to favor a benign outcome (like Ni simply filling pores) rather than producing unwanted phases. As an example of feedstock development, researchers have used polymer-coated metal powders to create a homogeneous distribution. Enneti et al. [64] fabricated a WC–Co feed with even cobalt distribution to ensure uniform shrinkage during binder burn-out and sintering. Cermet feedstocks often mimic what is done in powder metallurgy. Use of bimodal powders for high packing and adding a transient eutectic-forming additive to help sinter at a lower temperature.

3.4. Fiber-Reinforced Ceramic Matrix Composites (CMCs)

Fiber-reinforced CMCs, such as SiC/SiC and C/SiC systems, represent an important class of ceramic-based composites that offer significantly improved fracture toughness and thermal shock resistance compared to monolithic ceramics [67]. These materials depend on extrinsic toughening mechanisms, including fiber bridging, pull-out, and crack deflection. This enables damage tolerance under mechanical and thermal loading conditions [68].

Additive manufacturing of CMCs remains considerably more challenging than that of monolithic ceramics or cermets. Key difficulties arise from the need to control fiber orientation, ensure uniform matrix infiltration, and achieve strong and compliant fiber–matrix interfaces. Current approaches include direct ink writing of short-fiber-reinforced ceramic slurries and pre-ceramic polymer routes, in which fibers are embedded in a printable polymer precursor and then pyrolyzed. In some cases, hybrid methods combining AM with post-infiltration techniques, such as polymer infiltration and pyrolysis (PIP), are employed to improve densification [69].

Compared to pure ceramics, the processing–structure–property relationships in CMCs are fundamentally different. While monolithic ceramics primarily depend on densification and flaw minimization, CMCs derive their performance from engineered interfaces and multi-phase interactions. This results in enhanced fracture resistance and reliability, particularly in high-temperature and thermal shock environments [69,70].

Due to these advantages, additively manufactured CMCs are being explored for advanced applications in aerospace and defense, including turbine components, thermal protection systems, and rocket nozzles, where conventional ceramics often fail due to brittleness. However, challenges related to scalability, fiber alignment control, and achieving full density continue to limit widespread adoption.

3.5. Pre-Ceramic Polymers

Another approach to manufacturing ceramics is to print a pre-ceramic polymer that can be converted to a ceramic via pyrolysis. Polymers such as polycarbosilanes, polysiloxanes, and polysilazanes can be cured or printed like plastics, then heat-treated to form silicon carbide, silicon oxycarbide, or silicon carbonitride ceramics, respectively. This process, often used in stereolithography, is attractive because it bypasses directly handling ceramic powders during printing. Eckel et al. [71] demonstrated a UV-curable liquid siloxane that could be 3D printed into complex shapes, then fired in an inert atmosphere to yield near-fully dense SiOC ceramics with no cracks. The main drawback is significant linear shrinkage (~30%) during polymer-to-ceramic conversion, since the polymer loses mass (organics) and yields a ceramic char typically at 60–70% of the original volume. Cheype et al. [72] addressed this by using a polycarbosilane filled with SiC powder. During pyrolysis, the polycarbosilane yields SiC that bonds the pre-loaded SiC particles, resulting in a stoichiometric SiC part after one-step firing with much reduced shrinkage. Such techniques effectively embed the ceramic phase into the pre-ceramic polymer to minimize porosity and shrinkage. Pre-ceramic polymer feedstocks have been especially effective in DLP printing (due to the availability of UV-curable silicon resins). Table 3 lists common pre-ceramic polymers and their ceramic yields. The advantage of this approach is that it allows printing on relatively inexpensive photopolymer-based 3D printers, and the printed green parts are purely polymeric (hence easy to handle). However, careful pyrolysis schedules (slow heating rates, inert atmospheres) are required to avoid shape loss or cracking during the large mass loss in conversion. Also, the final microstructure of polymer-derived ceramics is often amorphous or nano-grained, which may limit high-temperature stability unless crystallized with additional heat treatment. The polymer-to-ceramic conversion process is accompanied by significant mass loss occurring from the decomposition of organic constituents and the release of volatile species. This results in volumetric shrinkage and densification. Thermodynamically, this transformation involves the transition from an organic polymer network to a ceramic structure with a higher atomic packing density, which contributes to dimensional reduction. Controlling heating rates and atmosphere is therefore critical to minimizing internal stresses and preventing cracking during pyrolysis [73].

Table 3. Pre-ceramic polymers and their pyrolysis products [71].

Pre-Ceramic Polymer	Chemical Backbone	Resulting Ceramic Phase
Siloxane	Si-O-Si	SiOC
Silazane	Si-N-Si	SiCN
Carbosilane	Si-C-Si	SiC
Siloxane-Silazane Composite	Si-O-Si + Si-N-Si	SiOCN

In summary, developing an optimal feedstock is a balancing act: powder characteristics (size, shape, distribution) must be matched with binder systems (polymers, dispersants, solvents) to achieve a printable mixture that still yields high ceramic content in the final part. With these feedstocks in hand, the next step after printing is to convert the "green" printed parts into fully dense ceramics through various post-processing and densification techniques.

4. Post-Processing and Densification

After a ceramic part is additively printed, it is typically in a "green" or intermediate state, containing binders or pores that must be removed to attain the desired density and properties. Post-processing is therefore crucial, and it usually involves one or more of the

following steps, including debinding, sintering (pressureless or assisted), and infiltration. The goal of post-processing is to eliminate organic material and porosity while avoiding the introduction of cracks or distortion. Each post-processing stage must be optimized for ceramic AM parts, which often have more complex shapes or internal features than conventionally pressed parts and thus can be more susceptible to non-uniform shrinkage or stress development. In this section, we describe the main post-processing strategies and recent advancements aimed at densifying additively manufactured ceramics, and discuss their effects on microstructure and final properties.

4.1. Debinding (Binder Removal)

Most printed ceramic parts contain significant amounts of organic binders (resins, polymers, or other processing additives) that must be removed before or during sintering. Debinding is often done by controlled heating, slowly raising the temperature to ~100–600 °C in air or an inert atmosphere to thermally decompose and evaporate the binder. It is critical to ramp the temperature slowly (typically 5–6 °C/min depending on part thickness [47,74]) so that volatile gases escape without building up pressure that could crack the part, though some researchers have recently tested ultra-fast debinding methods with heating and cooling rates up to 20 °C/min [75]. For vat-photopolymerized parts with high resin content, a two-stage debinding may be used. Initial low-temperature treatment to break down long polymer chains (reducing them to smaller fractions), followed by a higher temperature burn-out of the residue [76]. Non-oxide ceramics are typically debound in inert gas or vacuum to prevent oxidation. This often necessitates even slower heating rates, as observed by [47], for Si_3N_4, who used 0.1–5 °C/min to avoid internal oxidation while removing organics [77–79]. In some cases (e.g., delicate lattice structures), solvent debinding can be employed for a portion of the binder (e.g., leaching out a water-soluble binder phase before thermal debinding) to reduce the amount of material that must be burned out and thus mitigate defect risk [75]. Proper debinding leaves behind a fragile but intact porous ceramic structure, ready for sintering.

4.2. Pressureless Sintering

This is conventional furnace sintering at high temperature with no external pressure applied, relying on atomic diffusion to densify the ceramic part. Sintering parameters (peak temperature, hold time, heating rate, and atmosphere) are typically tuned to the ceramic material. For instance, alumina and zirconia are sintered in air at 1300–1700 °C for several hours [44,80], whereas highly temperature-resistant non-oxides may require higher temperatures (up to 2200 °C) or the presence of sintering aids to achieve densification [81]. In AM parts, one must account for anisotropic shrinkage. Printed layers or binder orientations might cause the part to shrink unevenly in different directions if unsupported, potentially introducing residual stresses or shape distortions. Bezek et al. found that increasing the sintering hold time and temperature for binder-jetted silica parts improved final density and flexural strength, but also led to more isotropic shrinkage (since the part had more time to equilibrate) [74]. In general, higher sintering temperatures and longer holds increase density and grain growth, which usually enhances strength up to a point, but excessive grain growth can reduce strength or toughness. Many printed ceramics can reach ~95–99% of theoretical density with careful sintering, but some, especially those printed with large binder content or from very fine powders, may suffer <93% density if not optimized, as reported for certain vacuum-sintered zirconia parts (93% dense) vs. conventionally sintered ones (99% dense). To predict and compensate for sintering shrinkage, designers often scale up the digital model so that after the known shrinkage (e.g., ~15% linear contraction for a given feedstock) the part ends up at the intended dimensions.

4.3. Hot Pressing and Spark Plasma Sintering (SPS)

These are pressure-assisted sintering techniques used to achieve higher density at lower temperatures or shorter times than pressureless sintering. In hot pressing, the printed and debound ceramic is placed in a die (often graphite) and heated while applying uniaxial pressure (20–50 MPa or more). This can yield nearly fully dense parts with fine grain sizes, since the pressure helps eliminate pores. For example, hot pressing has been used on laser-sintered SiC to further densify it, achieving ~675 MPa strength and 18 GPa hardness, significantly better than without hot pressing [46]. However, hot pressing is limited to relatively simple shapes (the part must conform to a die). SPS, also known as field-assisted sintering, is a variant where pulsed DC is passed through a conductive die (and sometimes the part, if conductive) to heat it extremely rapidly (heating rates of 50–300 °C/min are common) [82]. SPS can sinter ceramics to high density in minutes rather than hours [83,84]. Bhandari et al. [75] demonstrated using SPS as the final step for DLP-printed zirconia, shrinking the total densification time to under 30 s at peak temperature (once heated) and still achieving ~99% density. The main mechanism in SPS is still particle diffusion aided by pressure (~50–70 MPa typically), though some studies suggest the rapid heating and potential electrical field effects may enhance diffusion or preferentially heat grain boundaries. One caution is that the rapid heating/cooling can induce thermal gradients. SPS tooling and part geometry must be configured to minimize these and avoid cracking. Overall, these techniques are very promising for ceramic AM, as they can densify parts that are otherwise difficult to sinter (like nanocomposite or multi-phase materials) with less grain growth. However, they are currently limited to relatively small parts and require expensive equipment.

4.4. Infiltration

In cases where a printed part remains porous after sintering (or if full sintering would require impractically high temperature), infiltration can be used to fill remaining porosity with a secondary material, often improving density and strength. For porous ceramic skeletons, common infiltrants include molten metals (e.g., silicon for SiC preforms to create reaction-bonded SiC, or copper for alumina to make cermets) and polymer precursors (which convert to glass or ceramic upon heating). For example, Cramer et al. [85] binder-jetted SiC and then infiltrated the porous part with a liquid polycarbosiloxane, which, upon pyrolysis, yielded additional SiOC ceramic, boosting density and strength after multiple infiltrations. Wu et al. [86] printed alumina via binder jetting and carried out a sequence of infiltration steps with different solutions, achieving a remarkable 44-fold increase in bending strength after fully infiltrating the open porosity with a glassy phase. Infiltration is typically performed by immersing the porous part in the infiltrant or drawing the infiltrant through under vacuum, followed by curing or firing to solidify it. While infiltration can eliminate virtually all open porosity, the presence of a secondary phase can alter the high-temperature performance or other properties (e.g., metal-infiltrated ceramics have lower maximum service temperatures). Still, for applications such as ceramic filters, armor, or biomechanical components, infiltration is a valuable tool for achieving the required strengths without subjecting parts to extreme sintering schedules [87].

In Table 4, we summarized typical conditions and purposes of these post-processing steps. The sequencing and combination of post-processing steps must be tailored to the specific process and material. To provide a more comprehensive understanding, Table 4 has been further expanded to include the key advantages and limitations associated with each technique. This allows for a clearer comparison of their applicability, benefits, and constraints in the context of ceramic and ceramic composite additive manufacturing. For instance, a stereolithography-printed part might require a carefully staged debinding to

avoid blistering, followed by sintering in two phases (one to remove silica, one to densify the ceramic), whereas a direct laser-melted part might skip directly to a mild anneal or hot isostatic pressing if nearly dense. Researchers are actively exploring faster or more efficient post-processing routes. One emerging idea is ultra-fast thermal processing, or using microwave-assisted sintering to heat the part rapidly and uniformly [88]. Microwave-assisted sintering has emerged as an effective alternative to conventional thermal processing for additively manufactured ceramics. Unlike conventional heating, microwave processing enables rapid and volumetric heating. This can significantly reduce processing time and improve energy efficiency. Several studies have demonstrated its application in AM-fabricated ceramics such as alumina and silicon carbide, where microwave-assisted debinding and sintering contribute to enhanced densification and reduced thermal gradients. This is particularly beneficial for additively manufactured components, where non-uniform heating during conventional processing can lead to defects such as cracking and distortion [89–91]. These methods can shorten cycle times from days to hours or minutes, which is significant for industrial scalability.

Having discussed how to transform printed ceramics into dense final components, we next consider the mechanical and functional properties achieved by additively manufactured ceramics using these processes, and how they compare them to traditionally made ceramics.

During post-processing, shrinkage and densification are often non-uniform due to layer-wise fabrication. This leads to anisotropic behavior in additively manufactured ceramics. Variations in binder distribution, particle packing, and thermal gradients can result in differential shrinkage. This can also lead to residual stresses and potential distortion or cracking. These effects are particularly pronounced in complex geometries and thick sections. Therefore, careful control of heating rates, support strategies, and sintering profiles is essential to minimize anisotropy and ensure dimensional stability [92].

Emerging post-processing approaches, including microwave sintering and flash sintering, have recently attracted attention due to their ability to significantly reduce processing time and energy consumption [93,94]. These techniques enable rapid densification through enhanced diffusion mechanisms but remain limited by challenges in uniform heating and scalability. Additionally, while SPS offers rapid densification and fine microstructure control, it is constrained by limited sample size and high equipment cost. Similarly, HIP can achieve near-full densification and reduce residual porosity, but requires high-pressure systems and is less suitable for complex geometries. These limitations highlight the need for scalable and cost-effective post-processing solutions in ceramic AM [95].

Table 4. Post-processing steps relevant to additive manufacturing.

Post-Processing Step	Purpose	Mechanism	Thermodynamic Conditions	Time Scale	Advantages	Disadvantages	References
Debinding	Remove organic binder from green part	Thermal decomposition of organic polymers	100–600 °C, 0.1–20 °C/min	Hours to Days	• Essential for binder removal • Enables defect-free sintering • Applicable to all AM processes	• Time-consuming • Risk of cracking due to gas evolution	[48,77–81]
Sintering	Fuse ceramic particles to increase density	Atomic diffusion	1000–2200 °C, 3–5 °C/min	Hours	• Achieves densification • Improves mechanical properties • Widely applicable	• High temperature • Shrinkage and distortion	[45,76,82,83]

Table 4. *Cont.*

Post-Processing Step	Purpose	Mechanism	Thermodynamic Conditions	Time Scale	Advantages	Disadvantages	References
Hot Pressing	Quickly improve density and microstructure	Grain boundary/lattice diffusion	1200–1800 °C, 10 °C/min, 30 MPa	Hours	• High density • Fine microstructure	• Limited geometry • Expensive setup	[96]
Spark Plasma Sintering	Quickly improve density and microstructure	Rapid heating via Joule effect, pressure enhanced diffusion	1200 °C, 50–300 °C/min, 70 MPa	Minutes	• Rapid densification • Lower temperature • Fine grains	• Limited sample size • High cost	[83,84]
Infiltration	Introduce a second phase to improve material properties	Infiltrant fills pores via capillary action or applied pressure	Room temperature, can be under vacuum	Hours to Days	• Reduces porosity • Enhances strength	• Introduces secondary phase • Alters high-temperature properties	[85,86]

5. Mechanical and Functional Properties of AM Ceramics

Additively manufactured ceramics, once properly densified, can exhibit mechanical properties approaching those of conventionally processed ceramics. Reported values for flexural strength in AM ceramics are often in the 500–800 MPa range for materials like alumina, zirconia, and SiC, with Vickers hardness on the order of 13–18 GPa. Fracture toughness, however, remains relatively low (e.g., 4–6 MPa·$\sqrt{m}$ for alumina or zirconia [97,98]; ~3.5 MPa·$\sqrt{m}$ for carbides [99]) because most AM ceramics have similar microstructures to sintered ceramics (fine-grained and flaw-sensitive). In terms of functional properties, these materials retain the excellent wear resistance, thermal stability, and electrical/optical characteristics inherent to the ceramic composition, though subtle differences in microstructure (like residual porosity or grain orientation) can have effects. In this section, we summarize the key properties of additively manufactured ceramics. Mechanical properties, including strength, toughness, hardness, and wear resistance; thermal properties like thermal conductivity and shock resistance; and other functional properties such as dielectric behavior, magnetic response, and biocompatibility. Where possible, data from AM-fabricated parts are compared with those of similar conventionally fabricated ceramics to highlight current achievements and remaining gaps.

5.1. Strength, Toughness, Hardness, Wear Resistance

Ceramics produced by AM can attain high strength and hardness when fully densified and when critical flaws are minimized. As noted, flexural strengths in the range of 500–800 MPa have been reported for a variety of materials:

- Stereolithography-printed and sintered alumina has shown flexural strength up to ~550 MPa under optimized processing conditions [52], comparable to those of traditionally pressed alumina. Similarly, a DLP-printed alumina in another study had compressive strengths exceeding 120 MPa [50]. However, lower strength values are often reported for other AM techniques due to residual porosity and processing limitations.
- Extrusion-printed or binder-jetted zirconia parts have achieved bending strengths on the order of 490–600 MPa and Vickers hardness ~11–12 GPa. For example, Chen et al. [97] made zirconia dental crowns by inkjet and measured long-term compressive strength comparable to conventionally machined zirconia, attributable to achieving high density and a favorable rough surface that promoted stress-induced phase transformation toughening.
- Silicon carbide and silicon nitride printed parts can also be very strong if densification is high. Zou et al. [46] reported hot pressing SLS-printed SiC to ~675 MPa

flexural strength and 17.9 GPa hardness. For Si_3N_4, ~700 MPa bending strength and ~14 GPa hardness were achieved with digital light processing, which is on par with conventional reaction-bonded Si_3N_4 [47].

The fracture toughness of AM ceramics generally remains in the single digits (in MPa·$\sqrt{m}$). Dense zirconia typically has the highest toughness (~5–6 MPa·$\sqrt{m}$ due to transformation toughening). Additively made zirconia parts have shown toughness in this range. For instance, Chen et al.'s printed zirconia implants around 5.8 MPa·$\sqrt{m}$ [97]. Alumina and carbides are lower (3–4 MPa·$\sqrt{m}$) [98,99]. Schlacher et al. [100] printed layered alumina/zirconia composites, which exhibited crack deflection at the layer interfaces, yielding thermal shock resistance improvements (related to toughness). Still, achieving toughness on par with fiber-reinforced or engineered microstructures of traditional ceramics is challenging.

AM ceramics generally inherit the wear resistance of their base material. For instance, Enneti et al. [64] found that binder-jetted WC–Co cermets had similar abrasive wear rates to conventionally sintered ones (a volume loss of ~3.7 mm^3 in a standardized high-stress abrasion test, versus ~3.3 mm^3 for conventional, a slight difference attributed to 1–2% residual porosity). In another study, Niu et al. [41] showed that additively manufactured eutectic ZrO_2–Al_2O_3 had exceptional wear resistance due to in-situ formed hard phases. Tribological properties (friction and wear) of printed ceramics are often comparable to traditional parts if density and grain structure are similar. For example, a robocast silicon carbide nozzle exhibited wear rates nearly identical to a conventionally sintered SiC nozzle in slurry jet tests [101]. The main wear concern would be if any residual binder or secondary phases (e.g., glassy phases from incomplete sintering) are present on grain boundaries, as these can slightly reduce wear resistance. Generally, once fully sintered, the wear performance is governed by the ceramic composition and microstructure, not the fabrication route.

In addition to transformation toughening in zirconia-based systems, several other toughening mechanisms have been explored in additively manufactured ceramics. Particle toughening achieved by incorporating secondary phases such as alumina or zirconia enhances crack deflection and stress redistribution. Whisker-reinforced ceramics can improve fracture resistance through crack bridging and pull-out mechanisms, although their use in AM is currently limited due to challenges associated with dispersion. Fiber-reinforced CMCs offer significant improvement in toughness by relying on mechanisms such as fiber bridging, debonding, and pull-out to resist crack propagation. Compared to monolithic ceramics, these composite systems provide better damage tolerance and are particularly suited for high-temperature and thermal shock environments. However, their additive manufacturing remains complex due to challenges in fiber alignment, interface control, and densification [102,103].

In summary, with proper processing, additively manufactured ceramics can meet the mechanical demands for many structural applications. They have high hardness and compressive strength, and flexural strengths reaching the level of standard sintered ceramics have been demonstrated for several materials. The data indicate that porosity is the primary factor that can diminish strength in AM parts; each ~1% of residual porosity can reduce strength significantly due to stress concentration at pores. Eliminating those defects through improved feedstocks or post-treatments (e.g., HIP) often restores strength to theoretical values predicted by porosity–strength models (e.g., the Gibson–Ashby or minimum solid area models for porous ceramics). Research continues to push these properties higher: for example, Balla et al. [40] reported that using nano-powders and optimized sintering, they achieved alumina bending strength over 600 MPa from stereolithography prints. However, reliability remains a concern. Bose et al. [16] pointed out that variability in strength is sometimes large for AM ceramics, with Weibull moduli often lower than for

pressed parts, indicating more scatter in flaw size or distribution. Improving uniformity (by better feedstock dispersion and homogeneous debinding/sintering) will translate to more consistent mechanical performance.

In addition to strength and hardness, the reliability of additively manufactured ceramics is often evaluated using Weibull statistics, which quantify the variability in fracture strength due to flaw distribution. Compared to conventionally processed ceramics, AM ceramics may exhibit lower Weibull modulus values, reflecting greater variability associated with process-induced defects such as porosity and interlayer imperfections [104]. Furthermore, fatigue behavior remains a critical concern, particularly under cyclic loading conditions where microcracks can propagate from inherent defects. The relationship between porosity and strength is well established, with even small increases in porosity leading to significant reductions in mechanical performance. Therefore, improving densification and defect control is essential for enhancing both strength and reliability in ceramic AM components [105].

5.2. Thermal Properties

Ceramic materials are appreciated for thermal stability, and additively manufactured ceramics retain these properties, with some ability to tailor thermal behavior via microstructural design that AM enables.

A notable thermal property is thermal conductivity. Printed ceramics can be made with hierarchical porosity that yields low thermal conductivity for insulation, or conversely with oriented grains that provide high conductivity in a certain direction for heat dissipation. Dang et al. [106] printed alumina heat-sink structures with controlled mini-channel architectures and achieved efficient cooling performance, while also demonstrating that by introducing aligned microporosity, the effective thermal conductivity could be reduced for insulation purposes. Dutto et al. [107] fabricated graded porous ceramics by direct ink writing, where regions of higher porosity provided low conductivity (for insulation) and other regions were dense for structural support. By adjusting the pore size and distribution (through print pattern and ink formulation), they could tune thermal conductivity across a part by an order of magnitude.

Thermal shock resistance is another critical property for ceramics in high-temperature cycling. Additive manufacturing can create composite structures that improve thermal shock tolerance. For example, Qiu et al. [108] printed alumina with an in situ formed $MgAl_2O_4$ spinel second phase in a shell-like morphology around alumina grains. This "core-shell" microstructure (printable via careful slurry chemistry) acted to stop cracks: when a thermal shock induced a crack, the crack was blunted or deflected by the spinel phase, thereby doubling the thermal shock resistance compared to pure alumina. Similarly, Schlacher et al. [100] produced 3D-printed layered alumina–zirconia composites where the thermal expansion mismatch between layers induced crack deflection that dramatically improved resistance to thermal shock damage. These examples show that by using multi-material printing or controlled architecture, the inherent brittleness of ceramics under sudden temperature changes can be mitigated.

In terms of maximum use temperature and oxidation resistance, AM ceramics perform like conventional ones of the same composition. For instance, an additively manufactured SiC component will remain stable in air up to ~1600 °C (forming a protective SiO_2 scale) just as a conventionally made SiC would. If anything, the finer grain sizes often present in AM parts (due to shorter sintering times or use of nano-powders) could enhance oxidation slightly by providing faster diffusion paths, but also allow faster formation of a protective oxide.

AM also allows fabrication of heat exchangers and burners with optimized geometries: Hajimirzaee et al. [109] demonstrated an intricate catalytic converter substrate with enhanced conversion efficiency due to its 3D lattice, printed in a ceramic composite. These structures can sustain thermal cycling in engine exhaust conditions. They showed improved conversion after repeated cycles to 800 °C, indicating good thermal shock and chemical stability.

In addition to conventional oxide and non-oxide ceramics, ultra-high temperature ceramics (UHTCs) such as zirconium diboride (ZrB_2) and hafnium carbide (HfC) have attracted much attention due to their exceptional thermal stability in extreme environments. These materials exhibit melting points exceeding 3000 °C (HfC ~3900 °C) and maintain structural integrity under severe thermal loads. UHTCs also demonstrate relatively high thermal conductivity (e.g., ZrB_2 ~60–120 W/m·K), which helps reduce thermal gradients and improve thermal shock resistance compared to traditional ceramics. AM of UHTCs remains challenging due to their high melting temperatures and oxidation sensitivity, often requiring advanced techniques such as spark plasma sintering or reactive processing routes. However, recent developments highlight their potential for hypersonic vehicles, thermal protection systems, and rocket propulsion components [110,111].

In summary, thermal properties of AM ceramics largely mirror those of conventional ceramics, with the added benefit that AM enables microstructural engineering to enhance properties like thermal shock resistance or to achieve application-specific thermal conductivities. Additively manufactured ceramics have been successfully tested in high-temperature, high-heat-flux environments (such as rocket nozzles and diesel engine components) with performance matching conventional parts. As long as the part is sufficiently dense and free of large defects, its behavior under heat (whether insulating or structural) is dominated by the base ceramic's characteristics (phase composition, grain structure). The ability to incorporate porosity gradients or multilayer structures via AM is a unique advantage that can produce ceramic components optimized for thermal management in ways not possible before, bridging the gap between refractory performance and damage tolerance.

5.3. Electrical, Optical, and Biomedical Functionalities

Beyond structural roles, ceramics often serve functional purposes due to their electrical, magnetic, optical, or bioactive properties. AM is beginning to allow fine control over these properties by enabling complex shapes and heterogeneous material placement.

Electrical and Dielectric Properties: Some ceramics are used for their insulating or dielectric behavior (e.g., in RF components or as substrates for electronics). Printed ceramics generally have dielectric constants and losses comparable to conventionally made ones of the same purity. However, what AM offers is the ability to create geometrically complex dielectric structures (like porous metamaterials or tuned resonator arrays) that tailor electromagnetic response. Mei et al. [112] printed alumina composites with embedded SiC nanowires in controlled orientations. The SiC nanowires introduced dipolar polarization mechanisms, significantly increasing the dielectric loss tangent, effectively turning the printed object into an efficient microwave absorber. By adjusting the nanowire content spatially, they could make parts that absorb EM waves in certain regions but not others. Similarly, Balčas et al. [113] used a polymer/ceramic resin to print micro-optical elements that, after heat treatment, became a translucent glass-ceramic with a high refractive index, suitable for drone LIDAR systems. The fine 3D printing allowed fabrication of microlens arrays directly in a ceramic material, something traditionally done in polymer and then replicated.

Magnetic Properties: While ceramics are generally non-magnetic, certain printed ceramic composites (e.g., ferrites) can have designed magnetic responses. Chen et al. [114]

reported on 3D-printed impedance gradient materials where they embedded magnetic particles in a ceramic matrix via direct ink writing in a patterned way, achieving effective electromagnetic shielding that could be useful for stealth or electronics protection. Most magnetic applications of ceramics involve ferrites (e.g., NiZn ferrite for inductors), which have indeed been printed by methods like binder jetting and extrusion. The printed ferrites after sintering show permeability and permittivity in line with conventional ones, but again, the advantage is being able to integrate them into complex shapes or device architectures directly. For instance, 3D printed ferrite cores with intricate shapes for inductors have been demonstrated, showing Q-factors similar to standard cores but allowing novel coil winding geometries not possible before.

Optical Properties: Printed ceramics can be used to create optical components or photonic structures. By carefully controlling porosity and phase content, one can tailor the optical refractive index or absorption. For example, micro-porous alumina structures printed via phase separation can exhibit photonic bandgap effects or serve as diffusers with controlled scattering. Balčas et al. [113] mentioned the creation of high-index micro-optics (refractive index ~1.7) by printing a polymer that converts to a barium–silicate glass-ceramic. The fine 3D printed features were on the scale of a few microns, illustrating the precision achievable for optical devices such as microlens arrays or gratings. Another example is printing transparent alumina or yttria components: while fully dense alumina is not transparent due to porosity and grain boundaries, techniques like SPS post-processing (for example, on printed yttria parts) can produce translucent ceramics for optical windows.

Biocompatibility and Biomedical Integration: Ceramics, especially bio-ceramics like hydroxyapatite (HA) or zirconia, are heavily used in medical implants. AM enables customized implants, such as patient-specific bone scaffolds, with controlled porosity to encourage tissue ingrowth. Zhang et al. [115] demonstrated 3D-printed zirconia dental implants with intentionally roughened and porous surfaces (via controlled pore formation using inkjet methods) that significantly improved osteoblast adhesion and proliferation. The mechanical strength of such implants remained high (compressive strength > 150 MPa), and the osseointegration was enhanced by the porous topography in another study [116], leading to better bone attachment in vivo. Similarly, researchers like Vijayan et al. [117] discuss printing HA scaffolds with complex internal channels. These HA scaffolds can be designed to gradually biodegrade or release drugs, beyond what a conventionally molded HA part could do. HA is naturally osteoconductive, and printed HA parts have been shown to support bone cell activity and even deliver therapeutic agents.

Bioceramics like HA and tricalcium phosphate can also be printed as bone tissue scaffolds with precise pore architectures for vascularization. The advantage of AM here is clearly the geometric freedom to match patient anatomy and to include pore networks that mimic natural bone porosity. The biocompatibility of these printed ceramics is inherently high since the materials are the same as conventionally used ones; the printing process does not introduce any contamination if done properly (binder residues are burned out). For zirconia, which is inert in the body, printing allows customization of implant shape (for instance, a hip implant with a lattice structure on the bone-interfacing side to promote bone ingrowth). Clinical studies on printed porous titanium implants have shown improved integration; similarly, printed porous ceramic coatings on metal implants (like a lattice of HA on a Ti stem) are being developed to combine the toughness of metals with the bioactivity of ceramics.

In summary, AM extends the functional performance of ceramics by enabling complex shapes and multi-material structures that were previously unattainable. Electrically, it allows embedding conductive or high-loss phases in insulators for tailored dielectric properties; optically, it permits micro-structuring for lenses or photonic crystals; in the

biomedical realm, it provides patient-specific solutions and enhanced biointegration. These functional enhancements come without sacrificing the inherent advantages of ceramics. Printed ceramics still offer superb high-temperature performance, chemical inertness, and biocompatibility. As printing technologies mature, we expect to see more multifunctional ceramic components (for example, a single printed object that has a load-bearing dense core and a porous bone-contacting surface, or a microwave device that integrates a low-loss dielectric lattice with an absorbing layer in one monolithic print). The following section will discuss specific current applications of these technologies in various industries and how they are being implemented.

6. Applications in Mechanical Engineering Systems

AM of ceramics is beginning to transition from the lab to real-world applications across several engineering sectors. Here we survey applications in aerospace and defense, automotive, biomedical implants, and energy/electronics. In each domain, ceramics offer unique benefits (heat resistance, light weight, wear resistance, biocompatibility, etc.), and AM enables designs that capitalize on those benefits in ways not previously possible. We highlight current examples and case studies where additively manufactured ceramic components have been utilized or tested in practical mechanical engineering contexts, and discuss the advantages they provide.

6.1. Aerospace and Defense

The aerospace and defense industries stand to benefit greatly from ceramic AM because these sectors demand components that can withstand extreme conditions and often have complex shapes for optimized performance [118]. Rocket engines and hypersonic vehicles, for instance, use ceramic matrix composites for nozzles and thermal protection. NASA has initiated projects to develop additively manufactured ceramic rocket nozzle extensions, aiming to reduce cost and lead time by an order of magnitude compared to traditional fabrication [119]. One approach is using pre-ceramic polymer routes to print complex nozzle geometries, which can then be pyrolyzed into high-temperature ceramics like SiOC or SiCN. This yields the thermal stability of ceramics combined with the fabrication simplicity of polymer printing. Early tests have indicated these printed nozzles can indeed tolerate rocket exhaust environments, though long-term durability is still under evaluation.

Another aerospace application is lightweight high-temperature structures. Researchers have printed carbon fiber-reinforced SiC composites by extrusion, creating lightweight lattice structures for potential use in engine components or thermal shields [101]. These printed C/SiC parts had complex cellular geometries that offered an order-of-magnitude weight reduction while maintaining strength at high temperature. Defense applications have also explored ceramic AM for rapid field manufacturing of protective gear. For example, personal body armor plates made of alumina have been additively manufactured and tested against ballistic threats. Appleby-Thomas et al. [120] compared conventionally sintered vs. binder-jet printed alumina armor plates under live fire of armor-piercing rifle rounds (7.62 mm). Both types of plates successfully stopped the projectiles (shown in Figure 9), and the failure modes (localized ceramic fracture and bulging) were similar. The comparison demonstrates that additively manufactured ceramics can achieve performance comparable to conventionally produced counterparts, despite differences in internal structure. The additively manufactured plates showed slightly different fragment patterns due to their printed internal porosity distribution, but overall demonstrated that AM alumina armor can meet ballistic requirements. This capability suggests that in high-conflict or remote areas, armor or replacement ceramic components (for example, drone parts, missile radomes) could be manufactured on-demand with AM, bypassing lengthy supply chains.

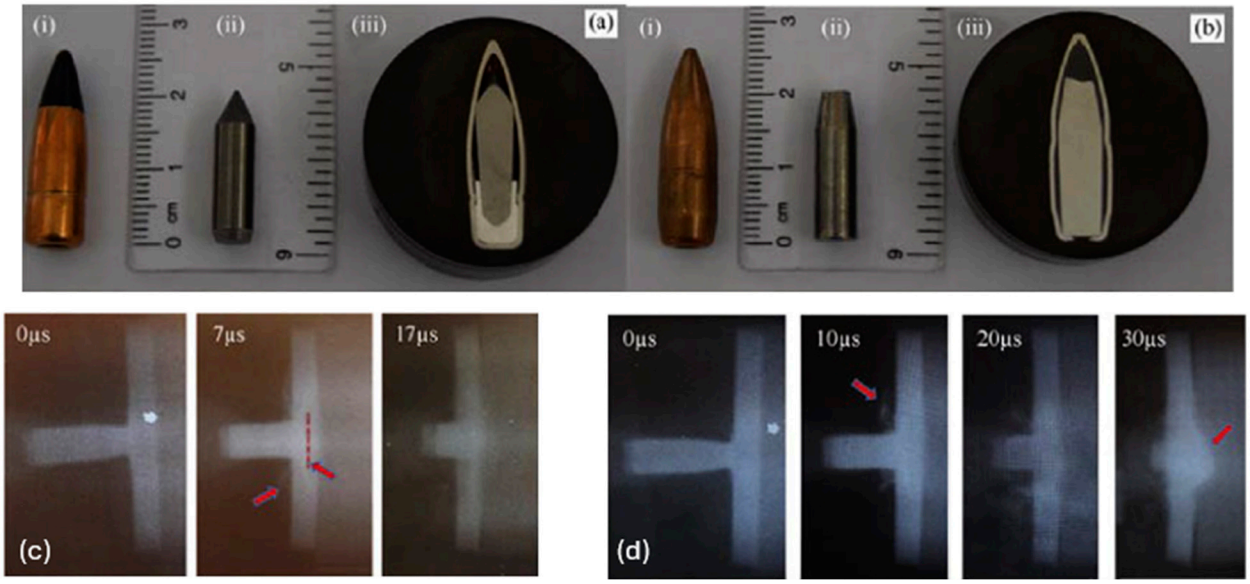


Figure 9. Ballistic behavior of additively manufactured alumina body armor. (**a**) Tungsten carbide-cobalt cored bullet and (**b**) steel-cored full metal jacket bullet. Both rounds are 7.62 × 39 mm (large rifle caliber) and armor-piercing. Panels i, ii, and iii refer to the full bullet, core, and cross section, respectively. (**c**,**d**) Impact frames of bullets on alumina body armor produced via conventional manufacturing (**c**) and AM (**d**). Both experiments show that the body armor can sufficiently stop the round. All panels appropriated from [120], open access.

In summary, in aerospace/defense, geometry freedom and weight reduction are the key drivers for ceramic AM adoption. Complex cooling channels in rocket nozzles, lattice-structured thermal shields, and on-demand production of spare parts (like UAV turbine blades or sensor housings) are all near-term use cases being actively developed. The high cost of mission-critical ceramic components (and the small production volumes) actually favor AM, since it can be more cost-effective for custom or limited-run parts. Ongoing qualification efforts are focusing on ensuring reliability (confidence in each printed part's performance), given the traditionally conservative nature of aerospace materials selection.

6.2. Automotive

The automotive industry is incorporating ceramic AM primarily in areas requiring high temperature and wear resistance. One example is in exhaust systems. Catalytic converter substrates and particulate filters are typically ceramic (cordierite or SiC) extruded in a honeycomb. AM allows more complex catalyst support geometries that improve flow mixing and surface area. Ceramics are also used in engine components like valves, seals, and fuel system parts for improved longevity. Additive manufacturing has produced parts such as silicon nitride valve guides and fuel pump plungers with internal cooling channels. Yang et al. listed various automotive ceramic components successfully made by AM, including bearings, seals, shafts, and turbocharger rotors, all of which exhibited increased temperature and corrosion resistance compared to steel equivalents [121]. For instance, a manufacturer printed a Si_3N_4 pre-chamber ignition component with an internal maze of channels that enhance flame propagation. This would be impossible to machine and test in a diesel engine, as it led to more complete combustion and survived the environment due to Si_3N_4's stability. These components take advantage of ceramics' ability to operate without lubrication or cooling where metals would fail, and AM's capacity to integrate complex cooling or aerodynamic features directly into the part.

Another promising application is to wear parts for heavy-duty vehicles. Brake pads and linings often incorporate ceramic particles. With AM, one can fabricate ceramic

composite brake components with novel patterns of material distribution for better performance (e.g., a gradient in hardness from the surface to the interior to balance wear and toughness). While most commercial brake rotors are still metallic, research has explored 3D-printed SiC-reinforced carbon disc brake prototypes, which drastically reduce fading at high temperatures [122].

In summary, in the automotive sector, ceramic AM enables more efficient, durable systems. Particularly notable is the ability to rapidly iterate designs of catalytic converters or engine components for performance gains, since prototypes can be printed rather than tooled. The environmental resistance of ceramics suits the trend towards high-efficiency, hot-running engines (including those in hybrid systems where exhaust temperatures can be higher). The acceptance of AM in automotive will hinge on demonstrating consistent performance in long-term tests and achieving production volumes. Given that catalytic converters and filters are produced in millions, the current AM is not yet scaled for that. However, for motorsports or specialty vehicles (where custom, optimized parts are valued), ceramic AM is already proving useful.

6.3. Biomedical Implants

Bioceramics are extensively used for dental and orthopedic implants, and AM is pushing the capabilities of personalized and improved implants. Zirconia dental implants are a prime example. Zirconia is often favored over metal implants for its tooth-like color and excellent biocompatibility (avoiding concerns with metal ions). Traditional zirconia implants are prefabricated in standard shapes. With AM, patient-specific zirconia implants can be made to precisely fit a patient's jaw anatomy or to include unique surface features. Zhang et al. [115] used inkjet 3D printing to create custom-shaped zirconia dental implants with an intentionally rough, porous surface layer. After sintering, the implants had densified cores for strength and a moderately porous outer surface (pore size tens of microns). In cell culture and animal tests, these AM zirconia implants showed enhanced osseointegration. Osteoblasts infiltrated and attached more readily to the porous surfaces, and bone-implant interfacial strength was higher than that of smooth implants. Mechanically, the printed zirconia (which was yttria-stabilized) retained high compressive strength exceeding the average bite forces, meaning no compromise in functionality for the patient.

Bone scaffolds and grafts made from HA or tricalcium phosphate are another critical application. With AM, scaffolds can be made porous in a controlled way to mimic trabecular bone and to guide tissue regeneration. Conventional bone grafts (often foams or granules) have random porosity, whereas AM scaffolds can have interconnected pore networks of any design (e.g., gyroid structures, radial gradients) [123].

Some ceramic AM in biomedicine goes beyond implants to devices. For instance, piezoelectric ceramics (like lead zirconate titanate, PZT) have been printed into lattice structures for biomedical sensors and showed similar piezoelectric coefficients as bulk PZT. This could lead to custom-shaped ultrasonic transducers or energy-harvesting implants that conform to the body [124].

While short-term in vitro and in vivo studies demonstrate promising biocompatibility, the long-term performance of additively manufactured ceramic implants remains an active area of research. Key considerations include long-term corrosion stability in physiological environments, potential inflammatory responses, and degradation behavior over extended periods. For instance, zirconia-based implants have shown excellent chemical stability and low ion release. This contributes to minimal inflammatory response over time, whereas calcium phosphate-based ceramics such as hydroxyapatite are designed to gradually degrade and integrate with surrounding bone tissue. However, long-term clinical data on addi-

tively manufactured ceramic implants are still limited, particularly regarding the effects of residual porosity and surface roughness introduced during the AM process [125,126].

Overall, ceramic AM in medicine enables patient-specific solutions that improve healing and reduce complications. We already see regulatory approvals for 3D-printed metal implants; ceramic implants are following, especially in dentistry. The key advantages are the tailor-made geometry (for aesthetics and fitness) and the ability to incorporate porosity or texture that stimulates biological integration (which is hard to do uniformly with machining or surface coatings). As patient demand grows for metal-free implants and as surgeons seek grafts that accelerate recovery, the use of 3D-printed bioceramics is expected to expand.

6.4. Energy and Electronics Applications

Ceramics play vital roles in energy systems and electronic devices, serving as insulators, catalysts, ionic conductors, etc., and AM is opening new design avenues in these fields.

In energy conversion and storage: Solid oxide fuel cells (SOFCs) consist largely of ceramic materials (e.g., yttria-stabilized zirconia electrolytes, ceramic electrodes). Traditionally, these cells are planar; 3D printing has enabled integral, monolithic SOFC structures that combine cell elements in one print. Kostretsova et al. [127] reported a single-step 3D printing and co-sintering of an entire SOFC stack (electrolyte and electrodes). This streamlined fabrication allowed more complex electrode geometries (like wave structures to increase triple-phase boundary length). The printed cells performed comparably to multi-step fabricated cells but with far fewer manufacturing steps, highlighting efficiency improvements.

Ceramic heat exchangers and radiators are another energy application [128]. Because ceramics can handle very high temperatures and corrosive fluids, printed ceramic heat exchangers are being developed for concentrated solar power plants and high-efficiency power electronics cooling. Du et al. [129] printed a SiC heat exchanger with a complex fin array and demonstrated it in a solar thermal loop, demonstrating effective heat transfer under a variety of thermodynamic conditions and air flow rates. The geometry flexibility allows optimization of cooling channels in ways that outperform conventional straight channels, leading to more compact and efficient heat exchangers. Similarly, printed ceramic filters and mixers with embedded heating elements (like conductive meshes printed alongside insulating ceramic) have been made for chemical reactors, reducing part count by integrating multiple functions [130].

For electronics, one exciting use of ceramic AM is in creating electromagnetic (EM) devices with complex 3D structures. For instance, printed alumina or silica can serve as dielectric substrates for antennas or radar-transparent domes with graded permittivity to minimize reflections (so-called "radar stealth" properties). Also, electroceramic components like inductors, capacitors, and sensors can be integrated into printed circuit boards by printing the ceramic directly into the board shape. This yields unusual form factors, for example, a cylindrical capacitor array printed as a single piece with interdigitated electrode layers of a ceramic dielectric and a conductive phase [118,131].

On the electrochemical side, ceramics are used in batteries and capacitors (e.g., solid electrolytes, separators) [132]. 3D-printed porous ceramics are being trialed as battery cell architectures that allow high loading of active material while maintaining structural integrity. For example, a lattice of alumina can act as a scaffold for solid-state battery electrolytes or cathodes, improving ionic pathways [133].

In summary, the energy and electronics sectors leverage ceramic AM for its ability to create geometrically complex, multi-functional components that improve performance or integration. Whether it's a solid oxide fuel cell with a 3D electrode mesh, a heat exchanger with internal cooling optimized by topology, or a ceramic antenna with built-in filtering

structures, additive manufacturing uniquely meets these needs. As these industries push for higher efficiency and integration (think compact power systems or IoT devices with unusual form factors), the design freedom offered by ceramic AM will be increasingly valuable.

7. Challenges in Additive Manufacturing of Ceramics and Composites

While challenges such as porosity, cracking, and cost have been discussed in earlier sections in the context of specific processes, this section consolidates these issues to provide a unified perspective on the key barriers to industrial adoption of ceramic additive manufacturing. Despite considerable progress, there remain significant challenges to be surmounted before ceramic AM is widely adopted in industry. Many of these challenges mirror those in conventional ceramic processing, but some are exacerbated or uniquely presented in the additive context. Key issues include: (1) achieving fully dense, defect-free parts without shrinkage cracks; (2) ensuring uniform microstructures and reproducibility; (3) improving the cost-effectiveness and scalability of ceramic AM processes; and (4) addressing design limitations and reliability concerns for critical applications. In this section, we discuss each of these challenges in detail and outline ongoing and future efforts to overcome them.

7.1. Porosity, Shrinkage, and Cracking During Sintering

One of the foremost hurdles for ceramic AM is managing the changes that occur during the sintering densification of printed parts. After binder removal, printed ceramics are often ~40–60% dense "brown" parts that must be sintered to >95% density. This densification entails significant linear shrinkage (often 15–30%), which, if not uniform, can introduce internal stresses leading to cracking. Cracks commonly initiate when different regions of the part densify at different rates or times. Carazzone et al. [134] observed via in situ microscopy that cracks in sintering tend to form at constrained areas early in densification, then propagate as the part continues to shrink. To mitigate this, sintering profiles are being optimized. Slower heating through critical temperature ranges and holding at intermediate temperatures can allow pores to equilibrate and relieve mismatch strains. Additionally, sintering in supporting media (like embedding the part in a powder bed) is sometimes used to mechanically support complex shapes and reduce differential shrinkage.

Another approach to combat sintering-related defects is employing AM strategies that minimize required shrinkage. For example, using high green density feedstocks (e.g., nearly full-density green parts from SLM or DED) cuts down shrinkage to a few percent. However, in processes like binder jetting or stereolithography, significant shrinkage is inevitable. Carefully calibrated anisotropic scaling of the digital model (accounting for greater shrinkage in certain directions if, say, layers are oriented) can at least yield final dimensions correctly, but it does not by itself prevent cracking. Research in this area includes adding transient sintering aids to promote densification at lower temperatures and thus lower mismatch with unsintered regions. Yet such aids must be used judiciously to avoid compromising high-temperature properties [135].

Residual porosity is also a concern. Even small levels of porosity (<5%) can degrade mechanical strength and dielectric properties significantly. Many printed ceramics end up with some closed porosity if sintering isn't fully complete. Techniques like hot isostatic pressing (HIP, applying isostatic gas pressure at high temperature) can eliminate this final porosity, but HIP is an expensive batch process and not always accessible. Achieving near-theoretical density reliably with printing-alone or simplified post-processes is challenging. Innovations such as ultrafast sintering hold promise by densifying parts so quickly that grain growth is limited and perhaps cracking can be avoided via rapid pass-through problematic temperature ranges. However, implementing such ultrafast processes at scale and uniformity is non-trivial [136].

7.2. Achieving Uniform Microstructure and Defect-Free Parts

The layer-by-layer nature of AM, combined with complex feedstock compositions (multi-phase mixtures, binders, etc.), can lead to heterogeneities in the printed part. For instance, material extrusion might cause slightly higher density in regions where extrusion paths overlap, or stereolithography might cure slightly deeper at part edges than in the interior, leading to non-uniform binder content. Such microstructural non-uniformity can translate to warping or local weakness after sintering [137]. For example, incomplete binder removal (e.g., residual carbon in the core of a thick part) can act as a flaw or cause delamination if the interior expands differently from the surface upon heating. Feedstock-related issues like particle agglomeration can also create defect clusters. Given the complexity of ceramic AM feedstocks (often containing dispersants, monomers, multiple powders), ensuring a homogeneous mixture is challenging. Real-time monitoring and feedback control during printing (e.g., measuring the drop mass in binder jetting or the cured layer thickness in SLA) is not yet fully developed for these processes, making quality assurance difficult [138].

Another frequent defect type is layer delamination or weak interlayer bonding, especially in extrusion and inkjet processes. If a layer dries too much before the next is deposited, bonding can be poor, manifesting as planar flaws after sintering. Maintaining optimal interlayer adhesion (through humidity control, rehydration steps, or minor binder re-melting for fusion) is an active area of process improvement [139].

Reproducibility of microstructure from one print to the next or from one machine to another is a recognized challenge. Bose et al. [16] pointed out that many studies report "successful" ceramic prints, but often do not discuss the consistency of the procedure, such as if only 1 out of 3 or 4 attempts was flawless. For industrial adoption, yields must be high. One cause of variability is the sensitivity of the feedstock condition. Slight sedimentation of a slurry or a few degrees change in resin temperature can alter viscosity and thus print outcome. Ensuring consistency thus requires strict feedstock handling protocols and possibly real-time rheology monitoring (which is currently not standard).

Defect detection in green bodies is also challenging. Porosity or cracks may be invisible until after sintering, when it's too late. Advanced imaging (e.g., micro-CT scanning of green parts) could catch internal flaws early, but doing this for every part is time-consuming. Improving in situ sensors on printers (like high-resolution cameras or layerwise IR imaging) could help detect anomalies during the build [140].

In summary, a big challenge is making sure every printed ceramic part is as uniform and defect-free as a well-pressed ceramic. Achieving that will likely involve improved material formulations (to reduce segregation and ensure even binder distribution), improved process control, and maybe machine learning to predict and adjust for sources of variation. Until these are resolved, critical applications may remain hesitant to use printed ceramics due to concerns about hidden defects.

7.3. Cost and Scalability Issues

Current ceramic AM processes can be expensive and relatively slow. High-end printers (e.g., large-format stereolithography or precision binder jetting machines) represent a significant capital cost, and many processes also require specialized post-processing furnaces (sometimes with controlled atmospheres). For production volumes, per-unit cost is often higher than traditional pressing or machining for simple geometries. For example, pressing thousands of alumina spark plugs is extremely cost-effective, whereas printing them might be an order of magnitude more expensive currently [141].

Another factor is material cost. Feedstocks like proprietary photopolymer slurries or very fine ceramic powders are expensive. Many AM processes also entail wasted auxiliary

material (e.g., unused powder in binder jetting or support materials in some DLP setups). Though powder can often be recycled, there can be degradation (e.g., resin contamination in unsintered powder or drying of slurries) [142]. Shahed et al. [51] noted that in binder jetting with bimodal powders, fine powders might segregate and become effectively unusable after a build, representing a loss. For more exotic ceramics (hafnium carbide, etc.), the cost of feedstock is a major barrier.

Scalability also remains an issue. Binder jetting can produce multiple parts in a build, but something like stereolithography typically produces one part or a small batch at a time. Long post-processing (multi-day debinding and sintering) further slows throughput. This is acceptable for aerospace or medical applications (low volume, high value), but is problematic for automotive or consumer electronics if large volumes are desired. Researchers are thus exploring ways to parallelize or speed up ceramic AM. For instance, using multiple inkjet heads to cover larger areas faster, or batch-printing many small parts in one go with support structures (akin to how many metal parts are printed on one build plate in laser sintering). However, packing parts can affect sintering uniformity due to part-to-part interactions (thus requiring careful spacing and sintering schedules) [31].

Another challenge is integration into existing manufacturing lines. Many companies have established processes for ceramics. Adopting AM might require retraining staff, adjusting QA protocols, and investing in new equipment. The initial cost and learning curve can deter adoption unless the benefits are very clear (e.g., impossible geometry or greatly reduced assembly steps) [130].

From a cost perspective, additive manufacturing of ceramics remains significantly more expensive than conventional processing for high-volume production. For example, binder jetting or stereolithography-based ceramic parts can cost approximately 2–5 times more per unit than traditionally sintered components when considering equipment, feedstock preparation, and post-processing steps. On top of this, build rates in ceramic AM are typically lower, further increasing the cost per part. However, for low-volume, highly complex, or customized components, AM can be economically competitive by eliminating tooling costs and reducing material waste. This trade-off highlights that while conventional manufacturing remains more cost-effective for mass production, additive manufacturing offers advantages in design flexibility and rapid prototyping [143].

In addressing cost and scalability, one focus is on automating post-processing. If debinding and sintering can be integrated into a continuous furnace rather than batch processes, throughput could improve. Some startups are exploring modular kiln designs where green parts enter one end and sintered parts exit continuously, potentially with conveyor systems that could handle fragile parts delicately (this is in early stages for ceramics). Another focus is reducing the need for support structures (since removing supports from dozens of tiny ceramic parts is labor-intensive), for example, through optimized build orientations or use of easily-removable support interfaces (like a layer of sacrificial material) [144].

7.4. Design Limitations and Reliability Concerns

While AM offers design freedom, it also has limitations in feature size and tolerance that must be recognized. For example, minimum feature sizes are on the order of tens of microns for stereolithography and binder jetting, and ~250 μm for extrusion-based processes. Extremely fine features (like sub-micron porosity or nano-scale surface patterns) are not achievable yet. Thus, designers must still work within a certain resolution grid. Moreover, some geometries can be printed but not survive post-processing; for instance, very thin walls may print well but crack during sintering due to a lack of support, or

large flat plates may warp. This requires a design mindset that accounts for the whole manufacturing cycle, not just the printing stage [144].

Reliability is a top concern for critical components. As noted, the variability in printed ceramics can be higher than in traditional ones. Bose et al. [16] emphasize that many published works do not report yield or statistical variation. For industrial acceptance, engineers will demand high Weibull moduli (a measure of reliability) for the mechanical properties of AM parts. Achieving this requires both uniform microstructures and consistent elimination of flaws. Any scattered flaw (like a local agglomerate or a stray void from an air bubble in a slurry) could become the origin of failure, and currently, the QA processes to catch those are not fully developed. Non-destructive evaluation of each ceramic AM part (e.g., by X-ray CT) might be necessary for applications like aerospace, adding to cost and time.

Another limitation is the lack of well-established design guidelines for ceramic AM. In metal AM, over the last decade, designers have learned what shapes tend to distort or how to include support structures. A similar knowledge base for ceramics is still forming. For example, a designer might not realize that a completely dense large ceramic part is likely to crack during sintering, whereas adding small, engineered porosities or splitting it into sections could alleviate that (counterintuitive to someone used to metals). The community is working on compiling these best practices. The development of simulation tools for ceramic AM (e.g., sintering simulation software such as MSC Simufact Additive) is also lagging behind metals and plastics. Tools that can predict shrinkage and stress in a complex printed geometry during firing would be extremely useful to refine designs before printing [16].

Finally, machine reliability for ceramics needs improvement. Many current ceramic AM machines are modified versions of polymer or metal printers and might not be optimized for the wear from ceramic particles (which are abrasive). Regular maintenance and part replacement (nozzles, recoaters, vats) add to cost and downtime. Purpose-built ceramic printers are emerging, but the field is small. With increased interest, we expect to see more robust equipment, e.g., extrusion systems with hardened nozzles and screws specifically for ceramic paste, or binder jet machines with improved powder handling to reduce clogging by fine ceramic dust [16].

8. Future Directions

The field of ceramic AM is rapidly evolving, and several emerging trends and research directions promise to expand its capabilities and mitigate current limitations. Key areas of development include: (1) multi-material and functionally graded ceramics, which can provide spatial variation in composition for tailored properties; (2) integration of artificial intelligence (AI) and machine learning (ML) to optimize designs and processes; (3) a growing emphasis on sustainability and recycling in ceramic AM to reduce waste and enable circular material use; and (4) advances in specific high-impact applications, notably in regenerative bioceramics and ultra-high-temperature aerospace ceramics. In this section, we discuss these future directions in detail, highlighting recent innovations and their implications for the next generation of ceramic AM.

8.1. Multi-Material and Functionally Graded Ceramic Composites

One exciting development is the prospect of printing ceramics with gradients in composition or structure, enabling properties that vary throughout a part. Traditional manufacturing finds it extremely difficult to produce functionally graded ceramics (FGCs), but AM can achieve it by changing feedstock during the building or by spatially programming material deposition. Scheithauer et al. at Fraunhofer IKTS have pioneered functionally graded porosity in ceramics using a multi-dispenser thermoplastic 3D print-

ing process [130,145,146]. They printed alumina parts that had well-defined regions of differing porosity (e.g., dense on one side, 50% porous on the other) as shown in Figure 10. These porosity gradients were used to create filters and mixers where certain sections need permeability, and others need strength. Additionally, by using multiple inkjet nozzles in their T3DP (Thermoplastic 3D Printing) system, they could deposit droplets of different ceramic compositions adjacently, yielding multi-material parts (e.g., an alumina part with embedded zirconia features) [147].

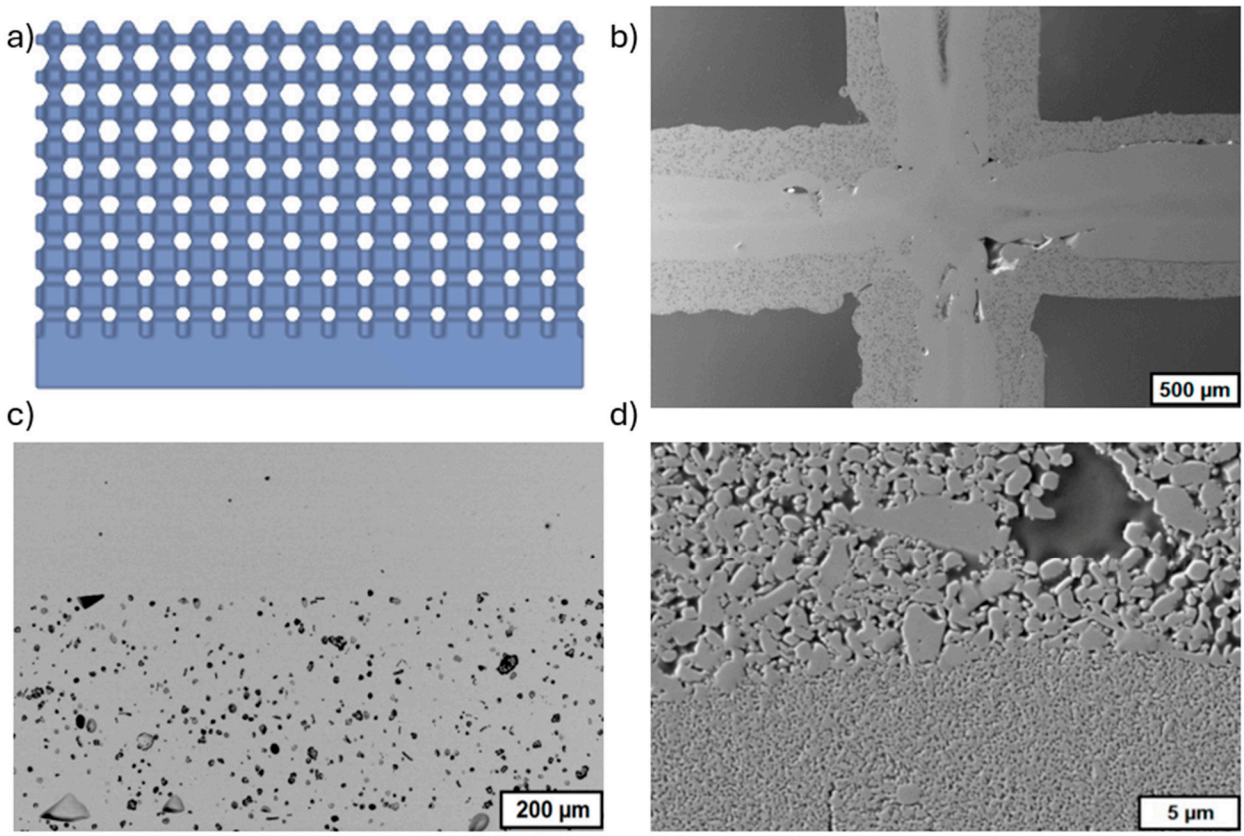


Figure 10. Additively manufactured ceramic structures demonstrating graded porosity. (**a**) Rendering of porosity gradient within a ceramic part; (**b**–**d**) SEM/FESEM images of interfaces between highly porous and less porous regions within additively manufactured ceramic parts. Appropriated from [145,146], open access.

Such multi-material capabilities open possibilities like ceramic tools with hard, wear-resistant exteriors and tough interiors, or thermal tiles with an outer ablative layer and inner insulating foam, all manufactured in one process. Already, they have demonstrated multi-material ceramic components such as graded catalytic reactors with integrated heating elements (ceramic with printed conductive tracks). Going forward, resolution is an area to improve. Current multi-material droplet printing yields millimeter-scale feature resolution, but research is pushing for finer control, possibly via laser-based methods that can fuse different ceramic powders in one bed.

Another angle is printing composites of ceramics with polymers or metals to achieve new functionality. For instance, embedding a metal mesh inside a printed ceramic can impart electrical conductivity for heating (think ceramic heaters or responsive shape-change materials when current passes through). With careful toolpath planning, one might print a continuous metal spiral inside a ceramic insulator structure. Recent work by Scheithauer et al. [130] on "heatable mixers," did essentially this, creating a ceramic mixer with an integrated molybdenum heating coil via multi-material printing.

8.2. Integration with AI and Machine Learning for AM Optimization

Artificial intelligence (AI) and machine learning (ML) are increasingly being applied to materials design and process optimization. For ceramic AM, which involves many complex variables (feedstock formulation, process parameters, shape complexities), AI/ML techniques are extremely promising in exploring the vast parameter space and improving outcomes. Wang et al. [148] categorize AI's impact on AM in three areas: design optimization, process control, and production management.

In the design stage, ML can assist in predicting which microstructural patterns or topology configurations will yield the best performance. Gu et al. [149] demonstrated an ML approach to optimize hierarchical composite microstructures, generating 100,000 random designs of bio-inspired composite structures, simulating them via finite element analysis (FEA), and training a deep neural network to predict mechanical properties from structure. This model could then rapidly search for billions of possibilities to suggest microarchitectures with high strength, which can be directly realized by AM. Such techniques could, for example, propose an optimal lattice design for a bone scaffold that maximizes strength while maintaining porosity, far faster than human trial-and-error. Other efforts have focused on integrating ML with CAD software (e.g., SolidWorks and Autodesk Fusion 360) to optimize topology during the solid modeling stage, increasing the accessibility of ceramics AM to inexperienced users [150].

In process optimization, ML models are being trained to correlate printing parameters with part quality. Caiazzo and Caggiano developed a neural network linking DED process parameters to the geometry of the melt pool (width, depth, height) [151]. By predicting melt pool geometry, their model helps avoid process regimes that lead to keyholing or unfused areas. Similarly, Tapia et al. created a Gaussian process model to predict final part porosity in DED based on input settings [152]. Although these examples are in metals, the approach translates to ceramics: an ML model could predict, for instance, the density or warpage of a sintered ceramic part based on factors like layer thickness, infill pattern, debinding rate, etc., allowing proactive parameter adjustments. The complexity of ceramics (with multiple phases and transformations) means multi-physics simulation is hard, but ML can learn from data and capture subtle interactions that might elude physical modeling.

Production and quality control can also benefit from AI and ML. Baturynska et al. [153] applied ML to improve dimensional accuracy across different printers by suggesting global scaling factors and corrections. Essentially, their system learned the systematic deviations between nominal and actual printed geometry and could then recommend adjustments to the design before printing to get the right final shape, which is extremely useful for compensation of shrinkage in ceramic sintering (a similar model might predict anisotropic shrinkage and auto-deform the input STL to counter it).

The overall vision is a closed-loop AM system where sensors gather data during printing and post-processing (e.g., layer images, temperature logs, shrinkage measurements), feed it to ML models, which then adjust parameters in real-time to ensure a good part. This could dramatically increase yield and consistency. Early steps of this are seen in some research setups (like using IR cameras and ML to adjust laser power in metal AM). In ceramics, perhaps a network could detect by layer 50 that a certain region is over-building (too much material) and instruct the printer to reduce binder dosing in that area for the remaining layers, preventing a local density peak that would crack in sintering.

AI is aiding materials discovery: for instance, generative models can propose new pre-ceramic polymer chemistries optimized for printability and ceramic yield, by training on past experiments. Or they could suggest an optimal mixture of three different particle sizes to maximize packing density based on known packing theories and iterative learning.

8.3. Sustainable Processing and Recycling

As AM matures, there is growing interest in making it more sustainable in line with circular economy principles. Ceramics manufacturing often involves high energy usage (for sintering) and can result in scrap or failed prints that are not easily recyclable (a sintered ceramic cannot be re-melted like a metal). However, several studies are addressing sustainability.

One area is recycling waste materials into ceramic feedstocks. For example, large amounts of industrial ceramic waste (like fly ash, slag, or even broken traditional ceramics) could be ground into powders and used in AM. Al Rashid and Koç reviewed polymer recycling in AM [154]; similarly, Singh et al. [155] combined recycled thermoplastics with ceramic fillers to print composite prototypes. The mechanical properties of parts from recycled feedstock were found to be equivalent to those made from virgin materials. Extending this idea, waste glass has been explored as a potential binder matrix in ceramic processing, or bio-based polymers could replace some synthetic binders [73].

Another push is minimizing waste during printing. Support structures and excess feedstock are a source of waste. Jiang et al. developed algorithms to optimize support structure geometry, reducing material usage by up to 40% for overhang supports [156]. In ceramics AM, one might use as little support as possible (since those support regions can introduce surface flaws during removal). There is also exploration of dissolvable supports in ceramics, e.g., printing support in a second material like salt or a low-melting glass that can be removed by bathing or thermal treatment, leaving no waste apart from a recyclable support material.

On the recycling front, some printed ceramic components (especially bio-ceramics) are biodegradable or resorbable, which is inherently sustainable for biomedical implants. But for structural ceramics, end-of-life recycling is tough. One concept is to grind down failed, or end-of-life, printed parts to reuse as powder. This is feasible if the ceramic is relatively pure and one can accept somewhat coarser powder (which might work for binder jetting). Kostretsova's single-step SOFC fabrication process also suggests manufacturing efficiency. By co-printing layers and co-sintering, they eliminate multiple firing steps, thus saving energy [127].

There is also interest in decentralized, on-demand production (as mentioned in defense). In terms of sustainability, on-demand local printing reduces the carbon footprint from shipping heavy, fragile ceramic parts around the world. If one can send a digital file and print in situ, it avoids transportation emissions and packaging waste [157].

Energy efficiency in the process itself is being tackled by those ultra-fast sintering techniques (like the 30-s SPS sintering example) [75], which drastically cut down energy consumption per part by shortening furnace time. Another method is using a microwave [88] or laser sintering, which can couple energy more directly into the part, potentially using less energy than heating an entire furnace.

Given regulatory and consumer pressure, demonstrating a lower environmental impact could become a selling point for AM. Already, companies note that AM produces less waste scrap than subtractive manufacturing (since you only use material where needed). For ceramics, while the scrap savings might be smaller in volume than for metal machining (which can remove a lot of material), the targeted use of expensive or scarce materials is a big advantage, e.g., printing only the amount of tantalum carbide needed for a part, rather than sintering a block and grinding away 80%.

8.4. Potential Breakthroughs in Biomedical and Aerospace Applications

Looking forward, some of the most groundbreaking applications of ceramic AM are likely in the biomedical and aerospace sectors.

In biomedicine, the integration of bioceramics with bioactive functionality and drug delivery is a frontier. Two recent studies printed hydroxyapatite implants designed not just to replace bone but to actively promote regeneration [116,117]. One created implant with controlled porosity and incorporated growth factors that encourage osteointegration (bone bonding) and angiogenesis (blood vessel formation). By precisely tuning pore size and surface area via AM, they achieved significant bone in-growth and vascularization into the implant, something prior porous implants struggled with if pore sizes were not optimal. A near-future breakthrough could be patient-specific load-bearing bone implants that also biodegrade at a rate matching natural tissue healing, effectively being replaced by the patient's own bone over time [158]. AM is essential here to get the complex geometry and internal structure. Another emerging idea is using ceramic scaffolds as localized drug delivery platforms: imagine a printed HA cage that slowly releases antibiotics or chemotherapy agents to a specific site (e.g., preventing infection in a large bone graft or targeting bone tumors). Vijayan et al. [117] review how apatite scaffolds can be loaded with drugs to fight infections (like antimicrobial peptides to protect an implant from bacteria). These multifunctional implants could revolutionize treatments by combining mechanical support and therapy delivery.

In aerospace, a major focus is on ultra-high-temperature ceramics (UHTCs) for next-generation propulsion and re-entry technologies. Materials like Ta_4HfC_5 (tantalum hafnium carbide) and ZrB_2–SiC composites are candidates for leading edges of hypersonic vehicles and rocket engine liners due to melting points in the range of 3500–4000 K [159,160]. Traditional manufacturing of these is extremely challenging (requiring hot pressing at >2000 °C). AM is being explored to shape UHTCs into complex coolant channel geometries or aerodynamic profiles. Kennedy et al. [161] have even printed ablative composite coatings (like silica-phenolic) using inexpensive commercial FDM machines, hinting at a future where a spacecraft's heat shield could be repairable or manufacturable on orbit or in remote sites.

Finally, as aerospace pushes toward reusable space vehicles and higher-speed flight, sensor integration in ceramic components (through multi-material AM) might allow real-time health monitoring of parts experiencing extreme environments. For example, printing a SiC leading edge with embedded sapphire fiber optics or piezoceramic sensors could allow it to report on its temperature, strain, or damage state during flight. AM is one of the only ways to embed such sensors in dense ceramics without compromising integrity.

9. Conclusions

AM of ceramics and ceramic-based composites has rapidly progressed from proof-of-concept to a technology capable of producing geometrically complex, high-performance components for a variety of engineering applications. In this review, we examined the major AM methods for ceramics, including stereolithography, binder jetting, material extrusion (robocasting), inkjet printing, powder bed fusion (SLS/SLM), and directed energy deposition, and discussed the feedstocks (oxide and non-oxide ceramics, cermets, pre-ceramic polymers) and post-processing strategies (debinding, sintering, hot pressing, infiltration) that convert printed "green" bodies into dense ceramic parts. We also surveyed the resultant properties of additively manufactured ceramics, which can include strengths in the 500–800 MPa range, hardness 13–18 GPa, and specialty functionalities like tailored thermal behavior or dielectric response. Notably, recent innovations have enabled multi-material grading, bioactive implants, and extremely high-temperature ceramics that were previously unattainable by traditional methods.

Continued innovation is expected to address the remaining challenges of ceramic AM. Issues of residual porosity, shrinkage cracking, and property variability are being

tackled through improved feedstock formulations (enabling higher green densities and uniform binder removal) and advanced sintering techniques (such as ultrafast or field-assisted sintering). The integration of machine learning for process control (e.g., real-time adjustment of build parameters or predictive compensation for shrinkage) is anticipated to greatly enhance consistency and yield. At the same time, emerging capabilities like multi-material printing and functionally graded structures will expand the design space for engineers, allowing single components to fulfill multiple roles (for instance, a load-bearing part that also has embedded sensing or a hard surface with a tough core).

The outlook for ceramic AM is bright. In aerospace and energy, the ability to create lightweight, heat-resistant parts with internal cooling or complex contouring will contribute to more efficient propulsion and thermal management systems. In biomedicine, patient-specific ceramic implants with improved osseointegration and drug-release functionalities are on the horizon, promising better outcomes in dental, orthopedic, and craniofacial reconstructions. These advances, coupled with a drive towards more sustainable and on-demand manufacturing, indicate that the role of ceramics AM will continue to grow.

Yet, some caution is warranted. Many promising results are currently at the laboratory or prototype stage. To fully realize ceramics AM in mainstream production, scalability and reliability must be proven. This will likely occur incrementally, first in high-value, low-volume sectors (aerospace, medical implants) where the advantages outweigh the costs, and later in broader industrial use as the technology matures and becomes more economical. Given the trajectory of research and the increasing commercial availability of ceramic 3D printers, it is reasonable to expect that within the next decade, additively manufactured ceramic components will become commonplace in specialized applications, and they will meet or exceed the performance of those made by traditional means.

Overall, ceramic AM is transforming what is possible in ceramic engineering. By combining the intrinsic merits of ceramics (such as high hardness, temperature stability, and biocompatibility) with the design freedom of AM, engineers can create solutions that were previously impractical or impossible. Continued interdisciplinary efforts focusing on feedstock science, process innovation, and intelligent control will further break down current barriers. As these challenges are overcome, ceramic AM is poised to move from an emerging technology to an established manufacturing option, empowering the next generation of high-performance, tailor-made ceramic components across industries.

Author Contributions: Conceptualization, S.A.J. and P.L.M.; Writing—original draft, S.A.J. and J.C.; Writing—review & editing, S.A.J. and P.L.M.; Supervision, P.L.M. All authors have read and agreed to the published version of the manuscript.

Funding: This research received no external funding.

Data Availability Statement: No new data were created or analyzed in this study.

Conflicts of Interest: The authors declare no conflicts of interest.

References

1. Dadkhah, M.; Tulliani, J.-M.; Saboori, A.; Iuliano, L. Additive Manufacturing of Ceramics: Advances, Challenges, and Outlook. *J. Eur. Ceram. Soc.* **2023**, *43*, 6635–6664. [CrossRef]
2. Findik, F. Review of High Temperature Materials. *Herit. Sustain. Dev.* **2023**, *5*, 213–228. [CrossRef]
3. Ćurković, L.; Žmak, I. Mechanical Properties and Applications of Advanced Ceramics. *Materials* **2024**, *17*, 3143. [CrossRef]
4. Wang, X.; Gao, X.; Zhang, Z.; Cheng, L.; Ma, H.; Yang, W. Advances in Modifications and High-Temperature Applications of Silicon Carbide Ceramic Matrix Composites in Aerospace: A Focused Review. *J. Eur. Ceram. Soc.* **2021**, *41*, 4671–4688. [CrossRef]
5. Elgazzar, A.; Zhou, S.-J.; Ouyang, J.-H.; Liu, Z.-G.; Wang, Y.-J.; Wang, Y.-M. A Critical Review of High-Temperature Tribology and Cutting Performance of Cermet and Ceramic Tool Materials. *Lubricants* **2023**, *11*, 122. [CrossRef]

6. Antony Jose, S.; Kasar, A.K.; Stanford, M.; Menezes, P.L. Unlocking Tribological Performance of Silver-Infused Cu-Al_2O_3 Self-Lubricating Cermet. *J. Tribol.* **2025**, *147*, 091107. [CrossRef]
7. Jose, S.A.; John, M.; Menezes, P.L. Cermet Systems: Synthesis, Properties, and Applications. *Ceramics* **2022**, *5*, 210–236. [CrossRef]
8. Ding, Z.; Deng, J.; Li, J.; Sun, G.; Ai, X. Wear Behavior of Ceramic Nozzles in Coal Water Slurry Burning. *Ceram. Int.* **2004**, *30*, 591–596. [CrossRef]
9. Zhang, W. A Review of Tribological Properties for Boron Carbide Ceramics. *Prog. Mater. Sci.* **2021**, *116*, 100718. [CrossRef]
10. Medvedovski, E. Influence of Corrosion and Mechanical Loads on Advanced Ceramic Components. *Ceram. Int.* **2013**, *39*, 2723–2741. [CrossRef]
11. Li, Y.; Wang, Q.; Zhu, W.; Ding, S.; Xing, L.; Bai, Z.; Wang, Y. Corrosion Characteristics and Mechanisms of Ceramic Coatings in Subcritical and Supercritical Aqueous Systems. *Ceram. Int.* **2025**, *51*, 19743–19760. [CrossRef]
12. Xiao, P. "Frontiers in Ceramics" Grand Challenges. *Front. Ceram.* **2023**, *1*, 1137377. [CrossRef]
13. Lakhdar, Y.; Tuck, C.; Binner, J.; Terry, A.; Goodridge, R. Additive Manufacturing of Advanced Ceramic Materials. *Prog. Mater. Sci.* **2021**, *116*, 100736. [CrossRef]
14. Olhero, S.M.; Torres, P.M.C.; Mesquita-Guimarães, J.; Baltazar, J.; Pinho-da-Cruz, J.; Gouveia, S. Conventional versus Additive Manufacturing in the Structural Performance of Dense Alumina-Zirconia Ceramics: 20 Years of Research, Challenges and Future Perspectives. *J. Manuf. Process.* **2022**, *77*, 838–879. [CrossRef]
15. Klocke, F. Modern Approaches for the Production of Ceramic Components. *J. Eur. Ceram. Soc.* **1997**, *17*, 457–465. [CrossRef]
16. Bose, S.; Akdogan, E.K.; Balla, V.K.; Ciliveri, S.; Colombo, P.; Franchin, G.; Ku, N.; Kushram, P.; Niu, F.; Pelz, J.; et al. 3D Printing of Ceramics: Advantages, Challenges, Applications, and Perspectives. *J. Am. Ceram. Soc.* **2024**, *107*, 7879–7920. [CrossRef]
17. Hinczewski, C.; Corbel, S.; Chartier, T. Ceramic Suspensions Suitable for Stereolithography. *J. Eur. Ceram. Soc.* **1998**, *18*, 583–590. [CrossRef]
18. Zhang, H.; Yang, Y.; Hu, K.; Liu, B.; Liu, M.; Huang, Z. Stereolithography-Based Additive Manufacturing of Lightweight and High-Strength Cf/SiC Ceramics. *Addit. Manuf.* **2020**, *34*, 101199. [CrossRef]
19. Chen, Q.; Juste, E.; Lasgorceix, M.; Petit, F.; Leriche, A. Binder Jetting Process with Ceramic Powders: Influence of Powder Properties and Printing Parameters. *Open Ceram.* **2022**, *9*, 100218. [CrossRef]
20. Hur, H.; Park, Y.J.; Kim, D.-H.; Ko, J.W. Material Extrusion for Ceramic Additive Manufacturing with Polymer-Free Ceramic Precursor Binder. *Mater. Des.* **2022**, *221*, 110930. [CrossRef]
21. Grossin, D.; Montón, A.; Navarrete-Segado, P.; Özmen, E.; Urruth, G.; Maury, F.; Maury, D.; Frances, C.; Tourbin, M.; Lenormand, P.; et al. A Review of Additive Manufacturing of Ceramics by Powder Bed Selective Laser Processing (Sintering/Melting): Calcium Phosphate, Silicon Carbide, Zirconia, Alumina, and Their Composites. *Open Ceram.* **2021**, *5*, 100073. [CrossRef]
22. Derby, B. Inkjet Printing Ceramics: From Drops to Solid. *J. Eur. Ceram. Soc.* **2011**, *31*, 2543–2550. [CrossRef]
23. Imran, M.M.; Che Idris, A.; De Silva, L.C.; Kim, Y.-B.; Abas, P.E. Advancements in 3D Printing: Directed Energy Deposition Techniques, Defect Analysis, and Quality Monitoring. *Technologies* **2024**, *12*, 86. [CrossRef]
24. Svetlizky, D.; Das, M.; Zheng, B.; Vyatskikh, A.L.; Bose, S.; Bandyopadhyay, A.; Schoenung, J.M.; Lavernia, E.J.; Eliaz, N. Directed Energy Deposition (DED) Additive Manufacturing: Physical Characteristics, Defects, Challenges and Applications. *Mater. Today* **2021**, *49*, 271–295. [CrossRef]
25. Griffith, M.L.; Halloran, J.W. Ultraviolet Curable Ceramic Suspensions for Stereolithography of Ceramics. In *Proceedings of the IMECE94; Manufacturing Science and Engineering: Volume 2—Non-Traditional Design and Layered Manufacturing; Rolling Technology; Intelligent Machine Tool Systems; Measurement and Inspection of Products and Processes; Non-Traditional Manufacturing Processes of the 1990s*; American Society of Mechanical Engineers: New York, NY, USA, 1994; pp. 529–534.
26. 3D Printing of Ceramics: A Review. *J. Eur. Ceram. Soc.* **2019**, *39*, 661–687. [CrossRef]
27. Watters, M.P.; Bernhardt, M.L. Modified Curing Protocol for Improved Strength of Binder-Jetted 3D Parts. *Rapid Prototyp. J.* **2017**, *23*, 1195–1201. [CrossRef]
28. Sarila, V.; Koneru, H.P.; Pyatla, S.; Cheepu, M.; Kantumunchu, V.C.; Ramachandran, D. An Overview on 3D Printing of Ceramics Using Binder Jetting Process. *Eng. Proc.* **2024**, *61*, 44. [CrossRef]
29. Lewis, J.A. Colloidal Processing of Ceramics. *J. Am. Ceram. Soc.* **2000**, *83*, 2341–2359. [CrossRef]
30. Spina, R.; Morfini, L. Material Extrusion Additive Manufacturing of Ceramics: A Review on Filament-Based Process. *Materials* **2024**, *17*, 2779. [CrossRef]
31. Ngo, T.D.; Kashani, A.; Imbalzano, G.; Nguyen, K.T.Q.; Hui, D. Additive Manufacturing (3D Printing): A Review of Materials, Methods, Applications and Challenges. *Compos. Part B Eng.* **2018**, *143*, 172–196. [CrossRef]
32. Lu, Z.; Xia, Y.; Miao, K.; Li, S.; Zhu, L.; Nan, H.; Cao, J.; Li, D. Microstructure Control of Highly Oriented Short Carbon Fibres in SiC Matrix Composites Fabricated by Direct Ink Writing. *Ceram. Int.* **2019**, *45*, 17262–17267. [CrossRef]
33. Romanczuk-Ruszuk, E.; Sztorch, B.; Pakuła, D.; Gabriel, E.; Nowak, K.; Przekop, R.E. 3D Printing Ceramics—Materials for Direct Extrusion Process. *Ceramics* **2023**, *6*, 364–385. [CrossRef]

34. Gao, B.; Zhao, H.; Peng, L.; Sun, Z. A Review of Research Progress in Selective Laser Melting (SLM). *Micromachines* **2022**, *14*, 57. [CrossRef]
35. Zhao, X.; Wang, T. Laser Powder Bed Fusion of Powder Material: A Review. *3D Print. Addit. Manuf.* **2023**, *10*, 1439–1454. [CrossRef]
36. Pal, R.; Basak, A. Linking Powder Properties, Printing Parameters, Post-Processing Methods, and Fatigue Properties in Additive Manufacturing of $AlSi_{10}Mg$. *Alloys* **2022**, *1*, 149–179. [CrossRef]
37. Zhang, J.; Zhu, H.; Liu, D.; Li, Y.; Huang, C. Piezoelectric Inkjet Printing: The Principles, Fluid Dynamics Challenges, and Applications. *Mater. Today Commun.* **2024**, *41*, 110866. [CrossRef]
38. Chen, P.-H.; Chen, W.-C.; Chang, S.-H. Bubble Growth and Ink Ejection Process of a Thermal Ink Jet Printhead. *Int. J. Mech. Sci.* **1997**, *39*, 683–695. [CrossRef]
39. Sireesha, M.; Lee, J.; Kranthi Kiran, A.S.; Babu, V.J.; Kee, B.B.T.; Ramakrishna, S. A Review on Additive Manufacturing and Its Way into the Oil and Gas Industry. *RSC Adv.* **2018**, *8*, 22460–22468. [CrossRef]
40. Balla, V.K.; Bose, S.; Bandyopadhyay, A. Processing of Bulk Alumina Ceramics Using Laser Engineered Net Shaping. *Int. J. Appl. Ceram. Technol.* **2008**, *5*, 234–242. [CrossRef]
41. Niu, F.; Wu, D.; Ma, G.; Wang, J.; Zhuang, J.; Jin, Z. Rapid Fabrication of Eutectic Ceramic Structures by Laser Engineered Net Shaping. *Procedia CIRP* **2016**, *42*, 91–95. [CrossRef]
42. Cho, K.T.; Nunez, L.; Shelton, J.; Sciammarella, F. Investigation of Effect of Processing Parameters for Direct Energy Deposition Additive Manufacturing Technologies. *J. Manuf. Mater. Process.* **2023**, *7*, 105. [CrossRef]
43. Miao, W.-J.; Wang, S.-Q.; Wang, Z.-H.; Wu, F.-B.; Zhang, Y.-Z.; Ouyang, J.-H.; Wang, Y.-M.; Zou, Y.-C. Additive Manufacturing of Advanced Structural Ceramics for Tribological Applications: Principles, Techniques, Microstructure and Properties. *Lubricants* **2025**, *13*, 112. [CrossRef]
44. Landek, D.; Ćurković, L.; Gabelica, I.; Kerolli Mustafa, M.; Žmak, I. Optimization of Sintering Process of Alumina Ceramics Using Response Surface Methodology. *Sustainability* **2021**, *13*, 6739. [CrossRef]
45. Yu, T.; Zhang, Z.; Liu, Q.; Kuliiev, R.; Orlovskaya, N.; Wu, D. Extrusion-Based Additive Manufacturing of Yttria-Partially-Stabilized Zirconia Ceramics. *Ceram. Int.* **2020**, *46*, 5020–5027. [CrossRef]
46. Zou, C.; Ou, Y.; Zhou, W.; Li, Z.; Zheng, P.; Guo, X. Microstructure and Properties of Hot Pressing Sintered SiC/Y3Al5O12 Composite Ceramics for Dry Gas Seals. *Materials* **2024**, *17*, 1182. [CrossRef]
47. Yang, P.; Sun, Z.; Huang, S.; Ou, J.; Jiang, Q.; Li, D.; Wu, S. Digital Light Processing 3D Printing of Surface-Oxidized Si_3N_4 Coated by Silane Coupling Agent. *J. Asian Ceram. Soc.* **2022**, *10*, 69–82. [CrossRef]
48. Kasar, A.K.; Menezes, P.L. Friction and Wear Behavior of Alumina Composites with In-Situ Formation of Aluminum Borate and Boron Nitride. *Materials* **2020**, *13*, 4502. [CrossRef] [PubMed]
49. Chan, S.S.L.; Sesso, M.L.; Franks, G.V. Direct Ink Writing of Hierarchical Porous Alumina-stabilized Emulsions: Rheology and Printability. *J. Am. Ceram. Soc.* **2020**, *103*, 5554–5566. [CrossRef]
50. Han, Z.; Liu, J.; Li, T.; Cao, Y.; Zhang, C.; Wang, Z. Dynamic Mechanical Properties of Alumina Prepared by Vat Photopolymerization Based on High Solid Loading Slurry. *Addit. Manuf.* **2025**, *97*, 104603. [CrossRef]
51. Shahed, K.S.; Groeneveld-Meijer, W.; Lear, M.; Schreiber, J.; Manogharan, G. Powder Spreading Behavior of Bimodal Ceramics in the Binder Jetting Process. *Mater. Sci. Addit. Manuf.* **2025**, *4*, 025110016. [CrossRef]
52. Rao, P.; Iwasa, M.; Kondoh, I. Properties of Low-Temperature-Sintered High Purity α-Alumina Ceramics. *J. Mater. Sci. Lett.* **2000**, *19*, 543–545. [CrossRef]
53. Rao, P. Preparation and Mechanical Properties of Al_2O_3–15wt.%ZrO_2 Composites. *Scr. Mater.* **2003**, *48*, 437–441. [CrossRef]
54. Liu, X.; Zou, B.; Xing, H.; Huang, C. The Preparation of ZrO_2-Al_2O_3 Composite Ceramic by SLA-3D Printing and Sintering Processing. *Ceram. Int.* **2020**, *46*, 937–944. [CrossRef]
55. Kuang, N.; Qi, H.; Zhao, W.; Wu, J. Influence of Resin Composition on the Photopolymerization of Zirconia Ceramics Fabricated by Digital Light Processing Additive Manufacturing. *Polymers* **2025**, *17*, 1354. [CrossRef]
56. Cramer, C.L.; Hmeidat, N.S.; Mitchell, D.J.; Snarr, P.L.; Cakmak, E.; Bullock, S.E.; Aguirre, T.G.; Martinez, M.C.; Armstrong, B.L. Rheology Improvement for Silicon Nitride and Resin Slurries for Vat Photopolymerization Printing and Sintering. *npj Adv. Manuf.* **2025**, *2*, 36. [CrossRef]
57. Bai, X.; Ding, G.; Zhang, K.; Wang, W.; Zhou, N.; Fang, D.; He, R. Stereolithography Additive Manufacturing and Sintering Approaches of SiC Ceramics. *Open Ceram.* **2021**, *5*, 100046. [CrossRef]
58. Tang, J.; Chang, H.; Guo, X.; Liu, M.; Wei, Y.; Huang, Z.; Yang, Y. Preparation of Photosensitive SiO_2/SiC Ceramic Slurry with High Solid Content for Stereolithography. *Ceram. Int.* **2022**, *48*, 30332–30337. [CrossRef]
59. Cao, J.; Miao, K.; Xiong, S.; Su, F.; Gao, D.; Lin, X.; Liu, Z.; Wang, P.; Liu, C.; Chen, Z. 3D Printing and in Situ Transformation of SiCnw/SiC Structures. *Addit. Manuf.* **2022**, *58*, 103053. [CrossRef]

60. Zou, R.; Bi, L.; Huang, Y.; Wang, Y.; Wang, Y.; Li, L.; Liu, J.; Feng, L.; Jiang, X.; Deng, B. A Biocompatible Silicon Nitride Dental Implant Material Prepared by Digital Light Processing Technology. *J. Mech. Behav. Biomed. Mater.* **2023**, *141*, 105756. [CrossRef]
61. Ding, G.; He, R.; Zhang, K.; Zhou, N.; Xu, H. Stereolithography 3D Printing of SiC Ceramic with Potential for Lightweight Optical Mirror. *Ceram. Int.* **2020**, *46*, 18785–18790. [CrossRef]
62. Kong, F.; Chen, X.; Li, Y.; Tian, L.; Zheng, F.; Wang, E.; Zhao, G. A Novel Approach to Prepare High Density SiC Ceramics by Powder Extrusion Printing (PEP) Combined with One-Step Sintering Method. *J. Eur. Ceram. Soc.* **2024**, *44*, 626–634. [CrossRef]
63. Li, S.; Lu, Z.; Zhang, H.; Ai, Z.; Ran, Y.; Li, Y.; Deng, X.; Li, D. Rheological Behavior of Multi-Sized SiC Inks Containing Polyelectrolyte Complexes Specifically for Direct Ink Writing. *J. Eur. Ceram. Soc.* **2022**, *42*, 4810–4816. [CrossRef]
64. Enneti, R.K.; Prough, K.C. Wear Properties of Sintered WC-12%Co Processed via Binder Jet 3D Printing (BJ3DP). *Int. J. Refract. Met. Hard Mater.* **2019**, *78*, 228–232. [CrossRef]
65. Davydova, A.; Domashenkov, A.; Sova, A.; Movtchan, I.; Bertrand, P.; Desplanques, B.; Peillon, N.; Saunier, S.; Desrayaud, C.; Bucher, S.; et al. Selective Laser Melting of Boron Carbide Particles Coated by a Cobalt-Based Metal Layer. *J. Mater. Process. Technol.* **2016**, *229*, 361–366. [CrossRef]
66. Vedel, D.; Storozhenko, M.; Mazur, P.; Konoval, V.; Skoryk, M.; Grigoriev, O.; Heaton, M.; Zavdoveev, A. Wetting and Interfacial Behavior of Fe, Co, Ni on (Ti, Zr, Hf, Nb, Ta)C High Entropy Ceramics. *Open Ceram.* **2023**, *15*, 100393. [CrossRef]
67. Cramer, C.L.; Yoon, B.; Lance, M.J.; Cakmak, E.; Campbell, Q.A.; Mitchell, D.J. Additive Manufacturing of C/C-SiC Ceramic Matrix Composites by Automated Fiber Placement of Continuous Fiber Tow in Polymer with Pyrolysis and Reactive Silicon Melt Infiltration. *J. Compos. Sci.* **2022**, *6*, 359. [CrossRef]
68. Wu, F.; Zhang, H.; Wu, C.; Sun, D.; Yuan, J.; Zhao, G.; Chen, Q.; Liu, Y. Study of Synergistic and Competitive Mechanisms on Toughening CFRP Composites with Intrinsic and Extrinsic Multiscale Interleaves. *Polymer* **2024**, *309*, 127429. [CrossRef]
69. Sharma, S.K.; Gajević, S.; Sharma, L.K.; Sharma, Y.; Sharma, M.; Milojević, S.; Savić, S.; Stojanović, B. From Processing to Performance: Innovations and Challenges in Ceramic-Based Materials. *Crystals* **2026**, *16*, 85. [CrossRef]
70. Bilsborough, J.; Neilsen-Burke, H.; Khatamifar, M.; Antunes, E. Review of Monolithic and Matrix Composite Ceramic Sandwich Structures for Integrated Thermal Protection in Hypersonic Vehicles. *Compos. Part B Eng.* **2025**, *307*, 112906. [CrossRef]
71. Eckel, Z.C.; Zhou, C.; Martin, J.H.; Jacobsen, A.J.; Carter, W.B.; Schaedler, T.A. Additive Manufacturing of Polymer-Derived Ceramics. *Science* **2016**, *351*, 58–62. [CrossRef]
72. Cheype, M.; Pateloup, V.; Bernard, S. Straightforward Design Strategy toward 3D Near-Net-Shape Stoichiometric SiC Parts. *Adv. Mater.* **2024**, *36*, 2307554. [CrossRef]
73. Colombo, P.; Mera, G.; Riedel, R.; Sorarù, G.D. Polymer-Derived Ceramics: 40 Years of Research and Innovation in Advanced Ceramics. *J. Am. Ceram. Soc.* **2010**, *93*, 1805–1837. [CrossRef]
74. Bezek, L.B.; Wilkerson, R.P.; Chad, J.L.; Quintana, T.E.; Patterson, B.M.; Adhikari, S.; Lee, K.-S. Evolution of Debinding and Sintering of a Silica-Based Ceramic Using Vat Photopolymerization Additive Manufacturing. *Addit. Manuf.* **2025**, *105*, 104795. [CrossRef]
75. Bhandari, S.; Manière, C.; Sedona, F.; De Bona, E.; Sglavo, V.M.; Colombo, P.; Fambri, L.; Biesuz, M.; Franchin, G. Ultra-Rapid Debinding and Sintering of Additively Manufactured Ceramics by Ultrafast High-Temperature Sintering. *J. Eur. Ceram. Soc.* **2024**, *44*, 328–340. [CrossRef]
76. Zhou, S.; Liu, G.; Wang, C.; Zhang, Y.; Yan, C.; Shi, Y. Thermal Debinding for Stereolithography Additive Manufacturing of Advanced Ceramic Parts: A Comprehensive Review. *Mater. Des.* **2024**, *238*, 112632. [CrossRef]
77. Wang, X.; Li, Y.; Liu, B.; Li, S.; Duan, W.; Wang, G.; Chen, F. Preparation of Si_3N_4 Ceramic Based on Digital Light Processing 3D Printing and Precursor Infiltration and Pyrolysis. *Int. J. Appl. Ceram. Technol.* **2023**, *20*, 1017–1027. [CrossRef]
78. He, R.; Ding, G.; Zhang, K.; Li, Y.; Fang, D. Fabrication of SiC Ceramic Architectures Using Stereolithography Combined with Precursor Infiltration and Pyrolysis. *Ceram. Int.* **2019**, *45*, 14006–14014. [CrossRef]
79. Li, M.; Huang, H.-L.; Wu, J.-M.; Wu, Y.-R.; Shi, Z.-A.; Zhang, J.-X.; Shi, Y.-S. Preparation and Properties of Si_3N_4 Ceramics via Digital Light Processing Using Si_3N_4 Powder Coated with Al_2O_3-Y_2O_3 Sintering Additives. *Addit. Manuf.* **2022**, *53*, 102713. [CrossRef]
80. Li, Y.; Sun, H.; Song, J.; Zhang, Z.; Lan, H.; Tian, L.; Xie, K. Effect of Two-Step Sintering on the Mechanical and Electrical Properties of 5YSZ and 8YSZ Ceramics. *Materials* **2023**, *16*, 2019. [CrossRef]
81. Lonergan, J.M.; Fahrenholtz, W.G.; Hilmas, G.E. Sintering Mechanisms and Kinetics for Reaction Hot-Pressed ZrB_2. *J. Am. Ceram. Soc.* **2015**, *98*, 2344–2351. [CrossRef]
82. Trapp, J.; Kieback, B. Fundamental Principles of Spark Plasma Sintering of Metals: Part I—Joule Heating Controlled by the Evolution of Powder Resistivity and Local Current Densities. *Powder Metall.* **2019**, *62*, 297–306. [CrossRef]
83. Anselmi-Tamburini, U.; Garay, J.E.; Munir, Z.A.; Tacca, A.; Maglia, F.; Spinolo, G. Spark Plasma Sintering and Characterization of Bulk Nanostructured Fully Stabilized Zirconia: Part I. Densification Studies. *J. Mater. Res.* **2004**, *19*, 3255–3262. [CrossRef]

84. Brucculeri, R.; Airoldi, L.; Baldini, P.; Vigani, B.; Rossi, S.; Morganti, S.; Auricchio, F.; Anselmi-Tamburini, U. Spark Plasma Sintering of Complex Metal and Ceramic Structures Produced by Material Extrusion. *3D Print. Addit. Manuf.* **2024**, *11*, e1246–e1256. [CrossRef]
85. Cramer, C.L.; Armstrong, H.; Flores-Betancourt, A.; Han, L.; Elliott, A.M.; Lara-Curzio, E.; Saito, T.; Nawaz, K. Processing and Properties of SiC Composites Made via Binder Jet 3D Printing and Infiltration and Pyrolysis of Preceramic Polymer. *Int. J. Ceram. Eng. Sci.* **2020**, *2*, 320–331. [CrossRef]
86. Wu, H.; Jiang, C.; Tang, C.; Wang, L.; Huang, S.; Ge, S.; Li, B.; Deng, X.; Wu, S. Binder Jetting Printed in Situ Mullite Strengthened Alumina Ceramics with Excellent Mechanical and Thermal Properties through Multi-Phase Infiltration. *Virtual Phys. Prototyp.* **2024**, *19*, e2427240. [CrossRef]
87. Kasar, A.K.; Jose, S.A.; D'Souza, B.; Menezes, P.L. Fabrication and Tribological Performance of Self-Lubricating Porous Materials and Composites: A Review. *Materials* **2024**, *17*, 3448. [CrossRef]
88. Curto, H.; Thuault, A.; Jean, F.; Violier, M.; Dupont, V.; Hornez, J.-C.; Leriche, A. Coupling Additive Manufacturing and Microwave Sintering: A Fast Processing Route of Alumina Ceramics. *J. Eur. Ceram. Soc.* **2020**, *40*, 2548–2554. [CrossRef]
89. Oghbaei, M.; Mirzaee, O. Microwave versus Conventional Sintering: A Review of Fundamentals, Advantages and Applications. *J. Alloys Compd.* **2010**, *494*, 175–189. [CrossRef]
90. Agrawal, D.K. Microwave Processing of Ceramics. *Curr. Opin. Solid State Mater. Sci.* **1998**, *3*, 480–485. [CrossRef]
91. Liu, Q.; Qiu, M.; Shen, L.; Jiao, C.; Ye, Y.; Xie, D.; Wang, C.; Xiao, M.; Zhao, J. Additive Manufacturing of Monolithic Microwave Dielectric Ceramic Filters via Digital Light Processing. *Electronics* **2019**, *8*, 1067. [CrossRef]
92. Zeng, Y.; Wang, J.; Liu, X.; Xue, Y.; Tang, L.; Tong, Y.; Jiang, F. Laser Additive Manufacturing of Ceramic Reinforced Titanium Matrix Composites: A Review of Microstructure, Properties, Auxiliary Processes, and Simulations. *Compos. Part A Appl. Sci. Manuf.* **2024**, *177*, 107941. [CrossRef]
93. Biesuz, M.; Sglavo, V.M. Flash Sintering of Ceramics. *J. Eur. Ceram. Soc.* **2019**, *39*, 115–143. [CrossRef]
94. Lin, M.-S.; Chu, K.-R. On the Non-Thermal Mechanisms in Microwave Sintering of Materials. *Materials* **2025**, *18*, 668. [CrossRef]
95. Guillon, O.; Gonzalez-Julian, J.; Dargatz, B.; Kessel, T.; Schierning, G.; Räthel, J.; Herrmann, M. Field-Assisted Sintering Technology/Spark Plasma Sintering: Mechanisms, Materials, and Technology Developments. *Adv. Eng. Mater.* **2014**, *16*, 830–849. [CrossRef]
96. Rong, Y.; Zhao, S.; Zhang, Q.; Qiao, J.; Sang, G.; Xi, X.; Yang, J. High-performance Alumina Composite Ceramics with Brick-and-mortar Structure Derived from Microsphere. *Int. J. Ceram. Eng. Sci.* **2025**, *7*, e70002. [CrossRef]
97. Chen, F.; Zhu, H.; Wu, J.-M.; Chen, S.; Cheng, L.-J.; Shi, Y.-S.; Mo, Y.-C.; Li, C.-H.; Xiao, J. Preparation and Biological Evaluation of ZrO2 All-Ceramic Teeth by DLP Technology. *Ceram. Int.* **2020**, *46*, 11268–11274. [CrossRef]
98. Snarr, P.L.; Jones, K.V.; Ghezawi, E.F.; Wereszczak, A.A.; Cramer, C.L. Apparent Fracture Toughness Estimation of Additively Manufactured Alumina from As-printed Chevron-notched Test Specimens. *J. Am. Ceram. Soc.* **2025**, *108*, e20327. [CrossRef]
99. Feng, K.; Hu, S.; Zhao, W.; Sun, J.; Mao, Y.; Cai, D.; Wu, J.; Wei, Q. Bimodal Powder Optimization in SiC Binder Jetting for Mechanical Performance. *Int. J. Mech. Sci.* **2024**, *274*, 109278. [CrossRef]
100. Schlacher, J.; Geier, S.; Schwentenwein, M.; Bermejo, R. Towards 3D-Printed Alumina-Based Multi-Material Components with Enhanced Thermal Shock Resistance. *J. Eur. Ceram. Soc.* **2024**, *44*, 2294–2303. [CrossRef]
101. Liu, K.; Qiu, L.; Zhang, Y.; Du, Y.; Sun, C.; Zhang, S.; Tu, R.; Wu, Y.; Sun, H.; Shi, Y. Additive Manufacturing of Continuous Carbon Fiber–Reinforced Silicon Carbide Ceramic Composites. *Int. J. Appl. Ceram. Technol.* **2023**, *20*, 3455–3469. [CrossRef]
102. Naslain, R. Design, Preparation and Properties of Non-Oxide CMCs for Application in Engines and Nuclear Reactors: An Overview. *Compos. Sci. Technol.* **2004**, *64*, 155–170. [CrossRef]
103. Becher, P.F. Microstructural Design of Toughened Ceramics. *J. Am. Ceram. Soc.* **1991**, *74*, 255–269. [CrossRef]
104. Danzer, R.; Supancic, P.; Lube, T. Failure Statistics Beyond the Weibull Behavior. In *27th Annual Cocoa Beach Conference on Advanced Ceramics and Composites: B: Ceramic Engineering and Science Proceedings*; John Wiley & Sons, Ltd.: Hoboken, NJ, USA, 2003; pp. 497–5026.
105. Härtelt, M.; Fünfschilling, S.; Schwind, T.; Riesch-Oppermann, H.; Fett, T.; Kruzic, J.J. Deducing the Fatigue Crack Growth Rates of Natural Flaws in Silicon Nitride Ceramics: Role of R-Curves. *J. Am. Ceram. Soc.* **2013**, *96*, 2593–2597. [CrossRef]
106. Dang, M.; Hu, S.; Zhou, G.; Yue, X.; Wang, S. 3D Printing of Alumina Ceramic Heat Sink with Mini-channels for Thermal Management. *Int. J. Appl. Ceram. Technol.* **2023**, *20*, 1371–1377. [CrossRef]
107. Dutto, A.; Zanini, M.; Jeoffroy, E.; Tervoort, E.; Mhatre, S.A.; Seibold, Z.B.; Bechthold, M.; Studart, A.R. 3D Printing of Hierarchical Porous Ceramics for Thermal Insulation and Evaporative Cooling. *Adv. Mater. Technol.* **2023**, *8*, 2201109. [CrossRef]
108. Qiu, Y.; Li, Q.; Yang, K.; Jin, F.; Fan, J.; Liang, J.; Zhou, Y.; Sun, X.; Li, J. Thermal Shock Resistant 3D Printed Ceramics Reinforced with MgAl2O4 Shell Structure. *J. Mater. Sci. Technol.* **2024**, *178*, 100–111. [CrossRef]
109. Hajimirzaee, S.; Shaw, D.; Howard, P.; Doyle, A.M. Industrial Scale 3D Printed Catalytic Converter for Emissions Control in a Dual-Fuel Heavy-Duty Engine. *Chem. Eng. Sci.* **2021**, *231*, 116287. [CrossRef]

110. Fahrenholtz, W.G.; Hilmas, G.E. Ultra-High Temperature Ceramics: Materials for Extreme Environments. *Scr. Mater.* **2017**, *129*, 94–99. [CrossRef]
111. Liu, Y.; Wang, H.; Hao, J.; Cheng, Y.; Dong, S.; Hu, P.; Han, W.; Zhang, X. Key Materials for Extreme High-Temperature Environments: Ultra-High-Temperature Ceramics and Their Composites. *Extreme Mater.* **2025**, *1*, 38–66. [CrossRef]
112. Mei, H.; Yang, D.; Yang, W.; Yao, L.; Yao, Y.; Cheng, L.; Zhang, L. 3D-Printed Impedance Gradient Al_2O_3 Ceramic with in-Situ Growing Needle-like SiC Nanowires for Electromagnetic Wave Absorption. *Ceram. Int.* **2021**, *47*, 31990–31999. [CrossRef]
113. Balčas, G.; Malinauskas, M.; Farsari, M.; Juodkazis, S. Fabrication of Glass-Ceramic 3D Micro-Optics by Combining Laser Lithography and Calcination. *Adv. Funct. Mater.* **2023**, *33*, 2215230. [CrossRef]
114. Chen, X.; Wang, W.; Su, R.; Huang, Y.; Li, Y.; He, R. 3D-Printed Electromagnetic Microwave Absorption Structures: A Comprehensive Review. *J. Mater. Chem. A* **2025**, *13*, 22240–22270. [CrossRef]
115. Zhang, F.; Spies, B.C.; Willems, E.; Inokoshi, M.; Wesemann, C.; Cokic, S.M.; Hache, B.; Kohal, R.J.; Altmann, B.; Vleugels, J.; et al. 3D Printed Zirconia Dental Implants with Integrated Directional Surface Pores Combine Mechanical Strength with Favorable Osteoblast Response. *Acta Biomater.* **2022**, *150*, 427–441. [CrossRef] [PubMed]
116. Feng, C.; Zhang, K.; He, R.; Ding, G.; Xia, M.; Jin, X.; Xie, C. Additive Manufacturing of Hydroxyapatite Bioceramic Scaffolds: Dispersion, Digital Light Processing, Sintering, Mechanical Properties, and Biocompatibility. *J. Adv. Ceram.* **2020**, *9*, 360–373. [CrossRef]
117. Vijayan, A.; Vishnu, J.; A, R.; Shankar, B.; Sambhudevan, S. A Review on Hydroxyapatite Fabrication: From Powders to Additive Manufactured Scaffolds. *Biomater. Sci.* **2025**, *13*, 913–945. [CrossRef] [PubMed]
118. Bai, L.; Gao, X.; Li, Y.; Li, Y.; Zhang, G. A Deep Insight into the Additively Manufactured Ceramics for Aerospace Applications. *ChemPhysMater* **2025**, *5*, 1–21. [CrossRef]
119. Valentine, P.; Gradl, P. Extreme-Temperature Carbon- and Ceramic-Matrix Composite Nozzle Extensions for Liquid Rocket Engines. In Proceedings of the 70th International Astronautical Congress, Washington, DC, USA, 21 October 2019; pp. 1–13.
120. Appleby-Thomas, G.J.; Jaansalu, K.; Hameed, A.; Painter, J.; Shackel, J.; Rowley, J. A Comparison of the Ballistic Behaviour of Conventionally Sintered and Additively Manufactured Alumina. *Def. Technol.* **2020**, *16*, 275–282. [CrossRef]
121. Yang, J.; Li, B.; Liu, J.; Tu, Z.; Wu, X. Application of Additive Manufacturing in the Automobile Industry: A Mini Review. *Processes* **2024**, *12*, 1101. [CrossRef]
122. Mutlu, I.; Eldogan, O.; Findik, F. Production of Ceramic Additive Automotive Brake Lining and Investigation of Its Braking Characterisation. *Ind. Lubr. Tribol.* **2005**, *57*, 84–92. [CrossRef]
123. Wang, Y.; Liu, Y.; Chen, S.; Siu, M.-F.F.; Liu, C.; Bai, J.; Wang, M. Enhancing Bone Regeneration through 3D Printed Biphasic Calcium Phosphate Scaffolds Featuring Graded Pore Sizes. *Bioact. Mater.* **2025**, *46*, 21–36. [CrossRef]
124. Gong, G.; You, Y.; Shen, H.; Laghaei, M.; Wang, Y.; Li, Y. 3D Printing Piezoelectric Materials: Innovations, Challenges, and Future Perspectives. *Mater. Today Sustain.* **2025**, *32*, 101257. [CrossRef]
125. Denry, I.; Kelly, J.R. State of the Art of Zirconia for Dental Applications. *Dent. Mater. Off. Publ. Acad. Dent. Mater.* **2008**, *24*, 299–307. [CrossRef] [PubMed]
126. Mirzaali, M.J.; Moosabeiki, V.; Rajaai, S.M.; Zhou, J.; Zadpoor, A.A. Additive Manufacturing of Biomaterials—Design Principles and Their Implementation. *Materials* **2022**, *15*, 5457. [CrossRef] [PubMed]
127. Kostretsova, N.; Pesce, A.; Anelli, S.; Nuñez, M.; Morata, A.; Smeacetto, F.; Torrell, M.; Tarancón, A. Single-Step Fully 3D Printed and Co-Sintered Solid Oxide Fuel Cells. *J. Mater. Chem. A* **2024**, *12*, 22960–22970. [CrossRef]
128. Hadian, A.; Morath, B.; Biedermann, M.; Meboldt, M.; Clemens, F. Selected Design Rules for Material Extrusion-Based Additive Manufacturing of Alumina Based Nozzles and Heat Exchangers Considering Limitations in Printing, Debinding, and Sintering. *Addit. Manuf.* **2023**, *75*, 103719. [CrossRef]
129. Du, W.; Yu, W.; France, D.M.; Singh, M.; Singh, D. Additive Manufacturing and Testing of a Ceramic Heat Exchanger for High-Temperature and High-Pressure Applications for Concentrating Solar Power. *Sol. Energy* **2022**, *236*, 654–665. [CrossRef]
130. Scheithauer, U.; Johne, R.; Gottlieb, L.; Weingarten, S.; Wiemer, H.; Holtzhausen, S. Recent Developments in the Field of Additive Manufacturing of Ceramic-Based Multi-Material Components Open the Door to Highly Functionalized Components. *Prog. Addit. Manuf.* **2025**, *10*, 4051–4059. [CrossRef]
131. Chietera, F.P. Additively Manufactured Antennas and Electromagnetic Devices. *Hardware* **2024**, *2*, 85–105. [CrossRef]
132. Chu, T.; Park, S.; Fu, K. 3D Printing-Enabled Advanced Electrode Architecture Design. *Carbon Energy* **2021**, *3*, 424–439. [CrossRef]
133. Randau, S.; Walther, F.; Neumann, A.; Schneider, Y.; Negi, R.S.; Mogwitz, B.; Sann, J.; Becker-Steinberger, K.; Danner, T.; Hein, S.; et al. On the Additive Microstructure in Composite Cathodes and Alumina-Coated Carbon Microwires for Improved All-Solid-State Batteries. *Chem. Mater.* **2021**, *33*, 1380–1393. [CrossRef]
134. Carazzone, J.R.; Bonar, M.D.; Baring, H.W.; Cantu, M.A.; Cordero, Z.C. In Situ Observations of Cracking in Constrained Sintering. *J. Am. Ceram. Soc.* **2019**, *102*, 602–610. [CrossRef]
135. Kakanuru, P.; Pochiraju, K. Simulation of Shrinkage during Sintering of Additively Manufactured Silica Green Bodies. *Addit. Manuf.* **2022**, *56*, 102908. [CrossRef]

136. Zuo, F.; Wang, Q.; Yan, Z.-Q.; Kermani, M.; Grasso, S.; Nie, G.-L.; Jiang, B.-B.; He, F.-P.; Lin, H.-T.; Wang, L.-G. Upscaling Ultrafast High-Temperature Sintering (UHS) to Consolidate Large-Sized and Complex-Shaped Ceramics. *Scr. Mater.* **2022**, *221*, 114973. [CrossRef]
137. Altıparmak, S.C.; Yardley, V.A.; Shi, Z.; Lin, J. Extrusion-Based Additive Manufacturing Technologies: State of the Art and Future Perspectives. *J. Manuf. Process.* **2022**, *83*, 607–636. [CrossRef]
138. Kim, J.; Choi, Y.-J.; Gal, C.W.; Park, H.; Yoon, S.-Y.; Yun, H. Effect of Dispersants on Structural Integrity of 3D Printed Ceramics. *Int. J. Appl. Ceram. Technol.* **2022**, *19*, 968–978. [CrossRef]
139. Staudacher, M.; Lube, T.; Schwarzer-Fischer, E.; Abel, J.; Reichel, M.; Lorenz, N.; Gottlieb, L.; Long, S.; Fehleisen, F.; Scheithauer, U. Strength Limiting Defects in Additively Manufactured Ceramics. *Open Ceram.* **2025**, *24*, 100858. [CrossRef]
140. Wu, X.; Teng, J.; Ji, X.; Xu, C.; Ma, D.; Sui, S.; Zhang, Z. Research Progress of the Defects and Innovations of Ceramic Vat Photopolymerization. *Addit. Manuf.* **2023**, *65*, 103441. [CrossRef]
141. Tofail, S.A.M.; Koumoulos, E.P.; Bandyopadhyay, A.; Bose, S.; O'Donoghue, L.; Charitidis, C. Additive Manufacturing: Scientific and Technological Challenges, Market Uptake and Opportunities. *Mater. Today* **2018**, *21*, 22–37. [CrossRef]
142. Gonzalez-Gutierrez, J.; Cano, S.; Schuschnigg, S.; Kukla, C.; Sapkota, J.; Holzer, C. Additive Manufacturing of Metallic and Ceramic Components by the Material Extrusion of Highly-Filled Polymers: A Review and Future Perspectives. *Materials* **2018**, *11*, 840. [CrossRef]
143. Zhou, L.; Miller, J.; Vezza, J.; Mayster, M.; Raffay, M.; Justice, Q.; Al Tamimi, Z.; Hansotte, G.; Sunkara, L.D.; Bernat, J. Additive Manufacturing: A Comprehensive Review. *Sensors* **2024**, *24*, 2668. [CrossRef]
144. Armstrong, M.; Mehrabi, H.; Naveed, N. An Overview of Modern Metal Additive Manufacturing Technology. *J. Manuf. Process.* **2022**, *84*, 1001–1029. [CrossRef]
145. Scheithauer, U.; Weingarten, S.; Johne, R.; Schwarzer, E.; Abel, J.; Richter, H.-J.; Moritz, T.; Michaelis, A. Ceramic-Based 4D Components: Additive Manufacturing (AM) of Ceramic-Based Functionally Graded Materials (FGM) by Thermoplastic 3D Printing (T3DP). *Materials* **2017**, *10*, 1368. [CrossRef]
146. Scheithauer, U.; Kerber, F.; Füssel, A.; Holtzhausen, S.; Beckert, W.; Schwarzer, E.; Weingarten, S.; Michaelis, A. Alternative Process Routes to Manufacture Porous Ceramics—Opportunities and Challenges. *Materials* **2019**, *12*, 663. [CrossRef]
147. Scheithauer, U.; Johne, R.; Weingarten, S.; Schwarzer, E.; Richter, H.-J.; Moritz, T.; Michaelis, A. Investigation of Droplet Deposition for Suspensions Usable for Thermoplastic 3D Printing (T3DP). *J. Mater. Eng. Perform.* **2018**, *27*, 44–51. [CrossRef]
148. Wang, C.; Tan, X.P.; Tor, S.B.; Lim, C.S. Machine Learning in Additive Manufacturing: State of the Art and Perspectives. *Addit. Manuf.* **2020**, *36*, 101538. [CrossRef]
149. Gu, G.X.; Chen, C.-T.; Richmond, D.J.; Buehler, M.J. Bioinspired Hierarchical Composite Design Using Machine Learning: Simulation, Additive Manufacturing, and Experiment. *Mater. Horiz.* **2018**, *5*, 939–945. [CrossRef]
150. Yao, X.; Moon, S.K.; Bi, G. A Hybrid Machine Learning Approach for Additive Manufacturing Design Feature Recommendation. *Rapid Prototyp. J.* **2017**, *23*, 983–997. [CrossRef]
151. Caiazzo, F.; Caggiano, A. Laser Direct Metal Deposition of 2024 Al Alloy: Trace Geometry Prediction via Machine Learning. *Materials* **2018**, *11*, 444. [CrossRef]
152. Tapia, G.; Elwany, A.H.; Sang, H. Prediction of Porosity in Metal-Based Additive Manufacturing Using Spatial Gaussian Process Models. *Addit. Manuf.* **2016**, *12*, 282–290. [CrossRef]
153. Baturynska, I.; Semeniuta, O.; Wang, K. Application of Machine Learning Methods to Improve Dimensional Accuracy in Additive Manufacturing. In *Advanced Manufacturing and Automation VIII*; Wang, K., Wang, Y., Strandhagen, J.O., Yu, T., Eds.; Lecture Notes in Electrical Engineering; Springer: Singapore, 2019; Volume 484, pp. 245–252.
154. Al Rashid, A.; Koç, M. Additive Manufacturing for Sustainability and Circular Economy: Needs, Challenges, and Opportunities for 3D Printing of Recycled Polymeric Waste. *Mater. Today Sustain.* **2023**, *24*, 100529. [CrossRef]
155. Singh, R.; Kumar, R.; Singh, I. Investigations on 3D Printed Thermosetting and Ceramic-Reinforced Recycled Thermoplastic-Based Functional Prototypes. *J. Thermoplast. Compos. Mater.* **2021**, *34*, 1103–1122. [CrossRef]
156. Jiang, J.; Xu, X.; Stringer, J. A new support strategy for reducing waste in additive manufacturing. In Proceedings of the 48th International Conference on Computers and Industrial Engineering (CIE 48), Auckland, New Zealand, 2–5 December 2018.
157. Bedi, P.; Singh, R.; Ahuja, I.P.S. Investigations for Tool Life of 3D Printed HDPE and LDPE Composite Based Rapid Tooling for Thermoplastics Machining Applications. *Eng. Res. Express* **2019**, *1*, 015003. [CrossRef]
158. Cinici, B.; Yaba, S.; Kurt, M.; Yalcin, H.C.; Duta, L.; Gunduz, O. Fabrication Strategies for Bioceramic Scaffolds in Bone Tissue Engineering with Generative Design Applications. *Biomimetics* **2024**, *9*, 409. [CrossRef]
159. Zhang, Z.; Williams, C.J.; Maddison, G.; Sha, Y.; Zhu, M.; Cheng, D.; Wei, C.; Zhong, X.; Liu, Z.; Mativenga, P.; et al. Laser Additive Manufacturing of Ultra-High Temperature Ta_4HfC_5 Ceramic Components. *J. Manuf. Process.* **2025**, *152*, 1051–1066. [CrossRef]

160. Aguirre, T.G.; Cramer, C.L.; Cakmak, E.; Lance, M.J.; Lowden, R.A. Processing and Microstructure of ZrB_2–SiC Composite Prepared by Reactive Spark Plasma Sintering. *Results Mater.* **2021**, *11*, 100217. [CrossRef]
161. Kennedy, A.; McNulty, Z.; Nutt, S. Producing Ablative Thermal Protection Systems by Additive Manufacturing. *Adv. Manuf. Polym. Compos. Sci.* **2024**, *10*, 2366622. [CrossRef]

Disclaimer/Publisher's Note: The statements, opinions and data contained in all publications are solely those of the individual author(s) and contributor(s) and not of MDPI and/or the editor(s). MDPI and/or the editor(s) disclaim responsibility for any injury to people or property resulting from any ideas, methods, instructions or products referred to in the content.